Supplement of Atmos. Meas. Tech., 15, 3353–3376, 2022
https://doi.org/10.5194/amt-15-3353-2022-supplement

Atmospheric Measurement Techniques
Open Access

Supplement of

Performance characterization of low-cost air quality sensors for off-grid deployment in rural Malawi

Ashley S. Bittner et al.

Correspondence to: Andrew P. Grieshop (apgriesh@ncsu.edu)

S1 Details of instrumentation

The ARISense sensor package is shown in Figure S1; see Cross et al. (2017) for full description. Version 2.0 added a GSM cell module and replaced the Ox-B421 with the Ox-B431 sensor (Alphasense Ltd., UK). The ARISense sensor packages used AC or DC power and drew 3 – 4 W on average. In rural Malawi, units relied on a DC power system of four 9-Watt solar panels and four 12,000mAh rechargeable batteries; batteries were in a separate weather-proofed housing with a single bus connected to the ARISense unit. Raw data were sampled every 60 seconds, integrated, and stored as daily data files on an internal USB drive. During deployment in Malawi, data files were periodically sent via email or uploaded to a shared Google Drive by an on-site local assistant using an Android phone.

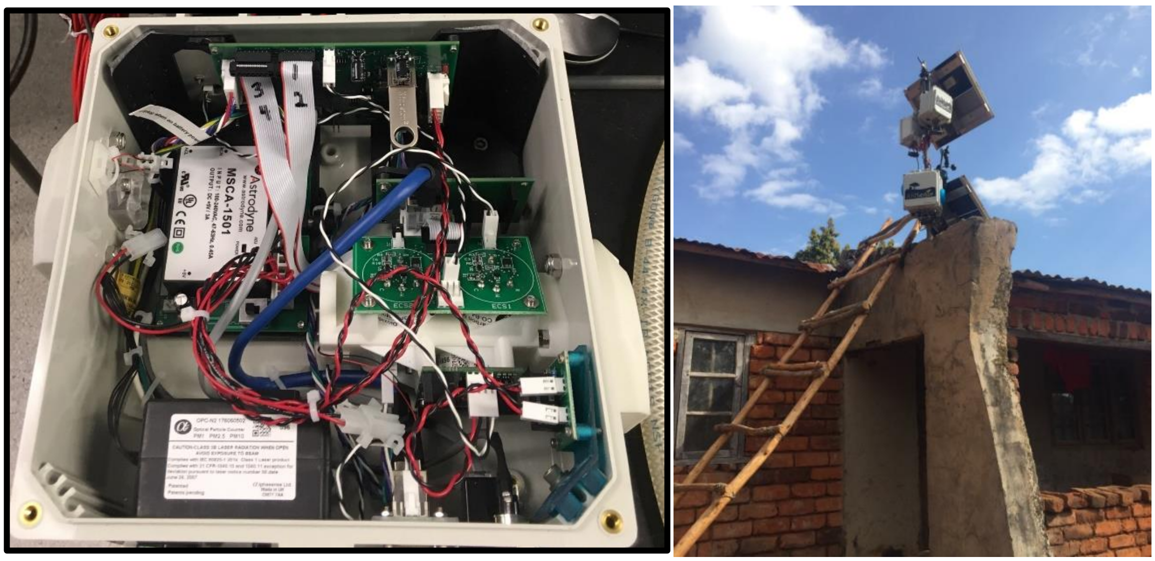

Figure S1: Image of ARISense (Version 1.0) interior (left), including integrated circuit board and internal data logging system. Image of ARISense in deployment setting (right) with solar panel power system mounted at Village 2 site in Mulanje, Malawi.

The MicroPEM uses a proprietary software to provide real-time mass concentration estimates from the nephelometer. We did not apply any correction factors and the internal slope was set to 1. The filters were equilibrated in a climate-controlled weighing chamber for 24 hours (22 ± 2 °C, 35 ± 2.5 % RH) and charge neutralized with Polonium and electrostatic ionization sources prior to pre- and post-weighing on an ultramicrobalance (Mettler Toledo UMX-2, 0.1 µg readability). Field handling blanks (N= 3) were collected in Malawi and were used to correct the gravimetric $PM_{2.5}$ concentrations. During field data collection, the filters were stored in sealed containers and were wrapped in foil to minimize exposure to light. The filters were stored in a refrigerator while in Malawi (when possible) and in the freezer after returning to the U.S. While in transit, the filters were at ambient temperature. The field blank-corrected gravimetric filter mass concentrations were used to post-correct the optical nephelometer readings.

S2 Details of pre-collocation in North Carolina

This study was conducted in 2017, before any standardized protocols were developed. The variable collocation periods used in this study were constrained by equipment malfunction, limited field personnel in Malawi, and international travel timelines. Recent U.S. EPA guidelines for supplemental air sensor performance assessment suggest 1) a minimum of 30 days (720 hours) of collocation, 2) two collocations during two different climatic seasons OR at two different sites, 3) a 24-hour averaging interval for the sensor and reference data, and 4) a 75% data completeness requirement (Duvall et al., 2021a, b).

Figure S2: Image of ARISense and reference instrumentation (left) at the Triple Oak monitoring site (right), North Carolina, USA. Image source: Google Earth Version 9.143.0.0 (May 1, 2018). *NC Collocation Site, Durham, NC, 27560 USA.* 35.865°N, 78.820°W. Borders and labels; places layer. Accessed: August 19, 2021. © Google Earth 2021. NC DEQ data available from: https://xapps.ncdenr.org/aq/ambient/AmbtSiteEnvista.jsp?site=371830021

S3 Description of assessment metrics and target values

Table S1: U.S. EPA recommended performance metrics and target values for low-cost gas (ozone) and particle sensor evaluation. Adapted from Tables ES-2 (Duvall et al., 2021a, b). ppbv = parts per billion by volume.

Performance Metric		**O_3 Target Value**	**$PM_{2.5}$ Target Value**
Precision	Standard deviation (SD) **OR**	≤ 5 ppbv	≤ 5 µg m^{-3}
	Coefficient of Variation (cV)	≤ 30%	≤ 30%
Bias	Slope (m)	1.0 ± 0.2	1.0 ± 0.35
	Intercept (b)	-5 ≤ b ≤ 5 ppbv	-5 ≤ b ≤ 5 µg m^{-3}
Linearity	Coefficient of Determination (R^2)	≥ 0.80	≥ 0.70
Error	Root Mean Square Error (RMSE)	≤ 5 ppbv	RMSE ≤ 7 µg m^{-3} **or** NRMSE ≤ 30%

The Coefficient of Determination (R^2) was used to assess linearity. For *n* measurements,

$$R^2 = 1 - \frac{\sum_{i=1}^{n}\left(c_{true,i} - c_{estimated,i}\right)^2}{\sum_{i=1}^{n}\left(\Delta c_{true,i}\right)^2} \tag{1}$$

where $c_{estimated,i}$ is the concentration as measured by the ARISense monitor, $c_{true,i}$ is the corresponding concentration measured by the reference instrument, and

$$\Delta c_{true,i} = c_{true,i} - \frac{1}{n}\sum_{j=1}^{n} c_{true,j} \tag{2}$$

The error in the ARISense measurements compared to the reference measurements was assessed using the Root Mean Square Error (RMSE):

$$RMSE = \sqrt{\frac{\sum_{i=1}^{n}\left(c_{estimated,i} - c_{true,i}\right)^2}{n}} \tag{3}$$

To assess precision, the Coefficient of Variation (cV) was used:

$$cV = \frac{\sqrt{\frac{\sum_{i=1}^{n}\Delta c_{estimated,i}^2}{n}}}{\frac{1}{n}\sum_{j=1}^{n} c_{estimated,j}} \tag{4}$$

where

$$\Delta c_{estimated,i} = c_{estimated,i} - \frac{1}{n}\sum_{j=1}^{n} c_{estimated,j} \tag{5}$$

To assess bias, we fit a linear regression model using the reference measurements as the independent variable or 'true' concentration and the ARISense measurements as the dependent variable or 'estimated' concentration and calculated the slope and intercept:

$$c_{estimated} = m * c_{true,i} + b \tag{6}$$

where m is the slope and b is the y-intercept.

For OPC-N2 measurements, prediction intervals were calculated for mean 1-hr averaged RH-corrected ambient $PM_{2.5}$ concentration measurements for each ARISense OPC-N2 using collocation data from ARI023 (Table 2) collected at the Village 2 site (Fig. 1d). Prediction intervals are a useful predictor to interpret future optical particle sensor readings collected after the evaluation period (Bean, 2021). We surmise statistical prediction intervals based off the collocation data of ARI023 can be used to interpret the 2017 ARISense data sets for the following reasons: a) we observed highly similar responses from the Alphasense OPC-N2 units in ARI013, ARI014, and ARI015 during pre-collocation in NC ($R^2 > 0.9$), b) this is the best-available in situ collocation data for our specific deployment conditions and source aerosol, and c) we only aimed to report low confidence level (1-sigma) prediction intervals with our measurements. Further, several studies have reported high OPC-N2 inter-unit agreement with a cV around 0.2 (Bulot et al., 2019; Crilley et al., 2018; Badura et al., 2018), although some review studies have shown low repeatability and reproducibility across Alphasense OPC-N2 units (Rai et al., 2017).

To estimate the interval for mean hourly averaged OPC-N2 measurements, we applied a Box-Cox transformation (Box and Cox, 1964) to a linear regression model using the ARI023 MicroPEM measurements as $c_{true,i}$ and the OPC-N2 measurements as $c_{estimated}$ to obtain an error term in the linear regression model independent of c_{true} and normally distributed, with zero mean and constant variance (Fig. S3b):

$$c_{estimated}(\lambda) = (c_{estimated}^{\lambda} - 1)/\lambda \tag{7}$$

where λ = -0.14. Interval estimates for mean hourly OPC-N2 measurements were calculated as prediction intervals:

$$c_{estimated}(\lambda) \pm t_{1-\frac{\alpha}{2},n-2}\sqrt{\frac{1}{n}\sum_{i=1}^{n}\left(c_{estimated,i} - c_{true,i}\right)^2 * (1 + \frac{1}{n} + (\frac{\Delta c_{true}(\lambda))^2}{\sum_{i=1}^{n}(\Delta c_{true,i})\hat{}2})} \tag{8}$$

where t is the t-statistic value for a given level of significance α.

(a)

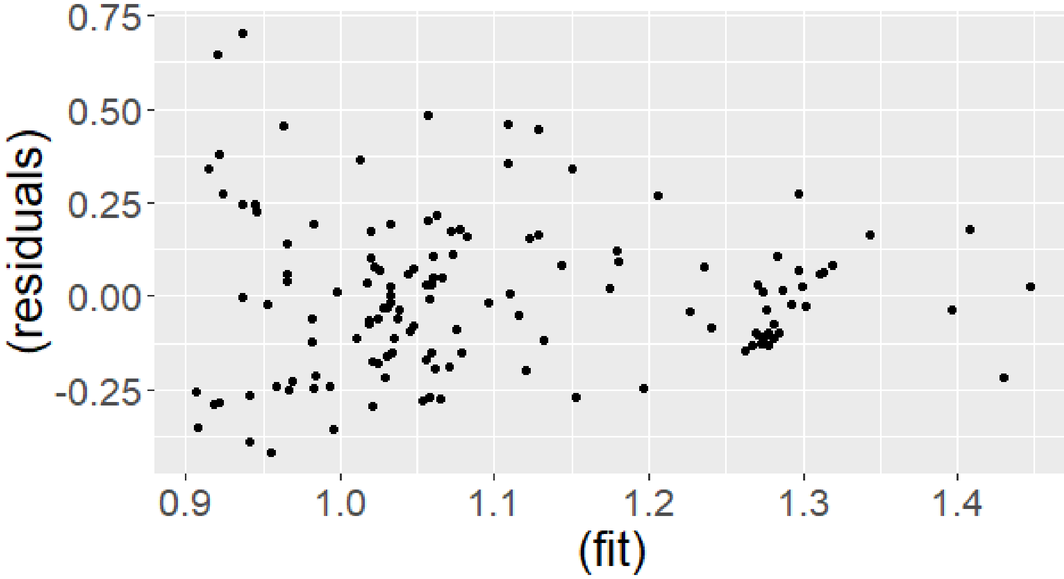

(b)

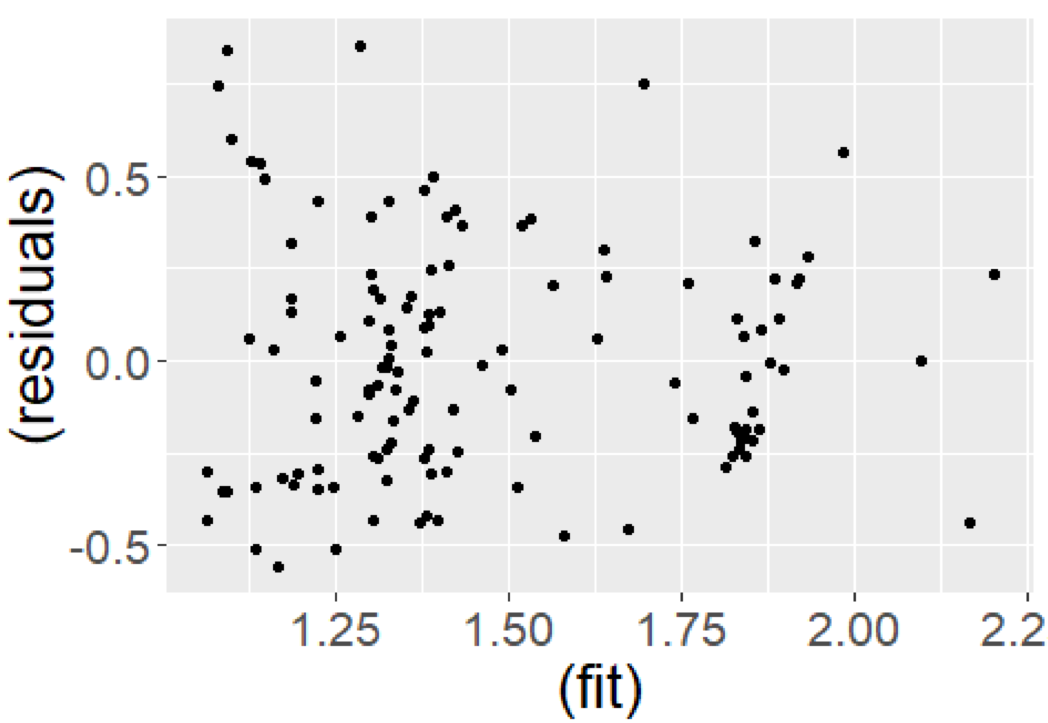

Figure S3: RH-corrected OPC-N2 $PM_{2.5}$ mass concentration (1-hr avg.) linear model residuals and fit range. Residuals = difference between OPC-N2 and MicroPEM measurements; (a) raw data, and (b) box-cox transformed data with outliers occurring from 3-6 AM local time (the morning cooking period) excluded. Original R Code (Bean, 2021).

The prediction intervals were reverse-transformed and used to estimate the range of mean hourly $c_{estimated}$ measurements. Outlying observations occurring between 3-6 AM were excluded for the fit to converge due to high ambient RH conditions (> 70%) coinciding with periods of fresh, biomass emissions from nearby morning cooking activity (Fig. S4). The analysis was completed in R (version 3.6.0) using RStudio (version 1.2.5042) with *MASS* (version 7.3-51.4) and *ggplot2* (version 3.3.2) libraries.

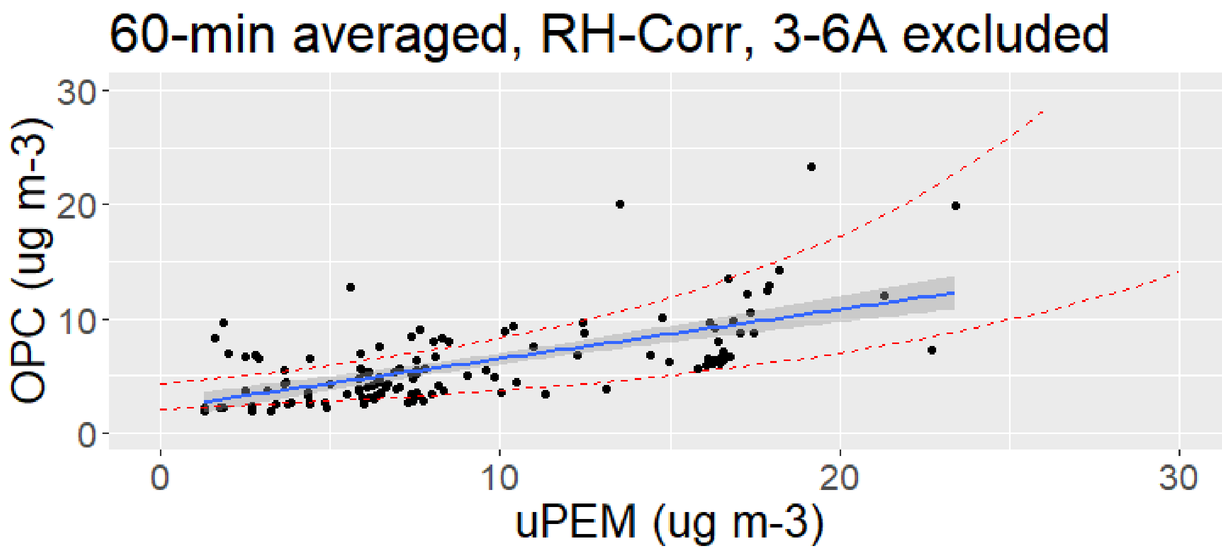

Figure S4: Alphasense OPC-N2 RH-corrected $PM_{2.5}$ mass concentration versus MicroPEM $PM_{2.5}$ concentration data used for the linear model; Fit line shown in blue, grey shaded area indicating 68% confidence interval in slope; Dotted red lines indicate 68% prediction interval upper and lower limits calculated from the linear model. Data are 60-min averaged. Data collected from 3-6 AM (morning cooking periods) were removed for the fit to converge. Original R Code (Bean, 2021).

S4 Satellite images of Malawi deployment sites

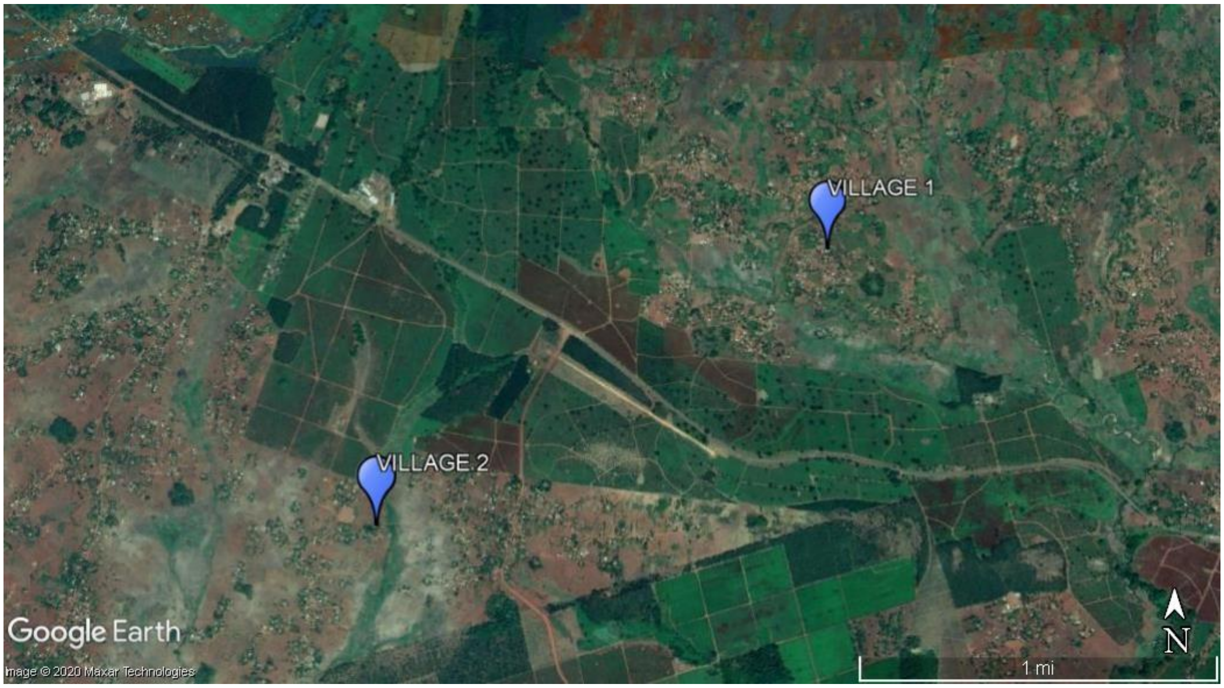

Figure S5: Satellite image of Mulanje "Village" sites (1 mile scale), blue markers indicate ARISense monitoring sites. Image source: Google Earth Pro Version 7.3.4.8248. *Mulanje, Malawi.* Borders and labels layer. Accessed: June 5, 2020. © Google Earth 2021.

Figure S6: Satellite image of “University” (1000ft scale), blue markers indicate low-cost monitoring sites. ARI015 was deployed to the University site and was mounted on the roof of an office building (7 m above ground) at the Bunda College of Agriculture in the Lilongwe University of Agricultural and Natural Resources near Lilongwe, Malawi for 382 days from 25 June 2017 to 13 July 2018. Image source: Google Earth Pro Version 7.3.4.8248. *Centre for Agricultural Research, Lilongwe University of Agriculture and Natural Resources, Bunda, Malawi.* 14.180°S, 33.774°E, eye elevation 1125 m. Borders and labels layer. Accessed: June 5, 2020. © Google Earth 2021.

S5 Details of high-concentration biomass burning emission experiments

Emissions measurement equipment, described in Champion and Grieshop (2019), placed near the emission sources directly in the plume measured mean CO concentrations of 50-300 ppb and maximum CO concentrations of 200-3800 ppm. In all experiments, the ARISense were placed further away (3-8 m) from the source. ARISense CO sensors saturated (at 5 ppm) for much of the testing period. Depending on the source type, these experiments ranged from 20-48 hours each. ARI013 was used for 3 experiments (75 hours total) and ARI014 was used for 4 experiments (100 hours total).

S6 Details of remote sensing data

MOPITT and MERRA-2 data were obtained for the Village and University sites. The resolution of the satellite observations meant that Village 1 and Village 2 fell within the same spatial cell. Given this, the Village 1 and Village 2 monthly mean measurements were averaged, and the "Village Mean" was used to compare to the remote sensing observations. The ARI015 data (University) was located far enough away and was dissimilar enough from the Village Mean data to be kept separate (Fig. S8).

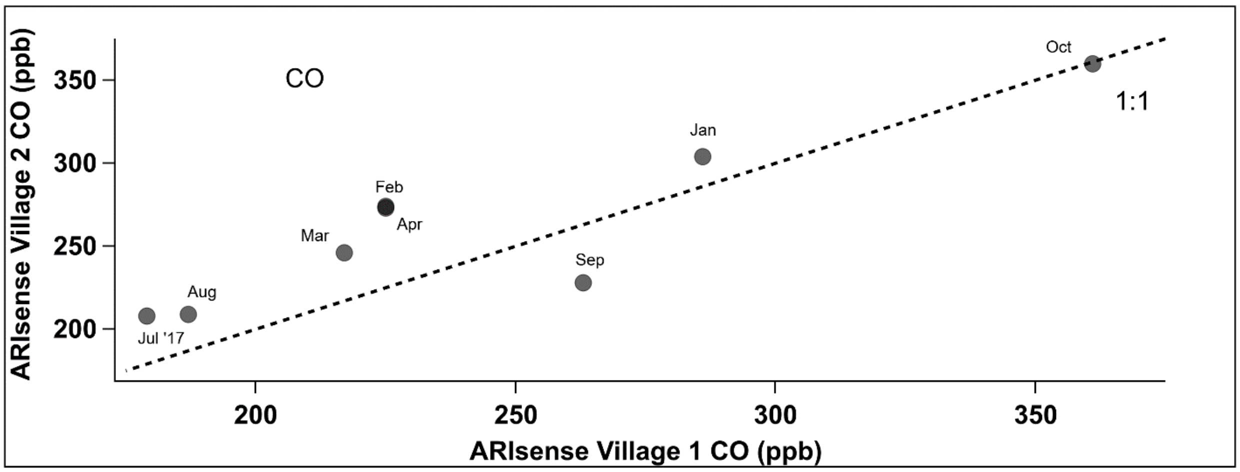

Figure S7: Scatter plot of Village 2 (y-axis) and Village 1 (x-axis) monthly mean CO concentration (calibrated with the kNN Hybrid model). A one-to-one line is shown as the dotted black line.

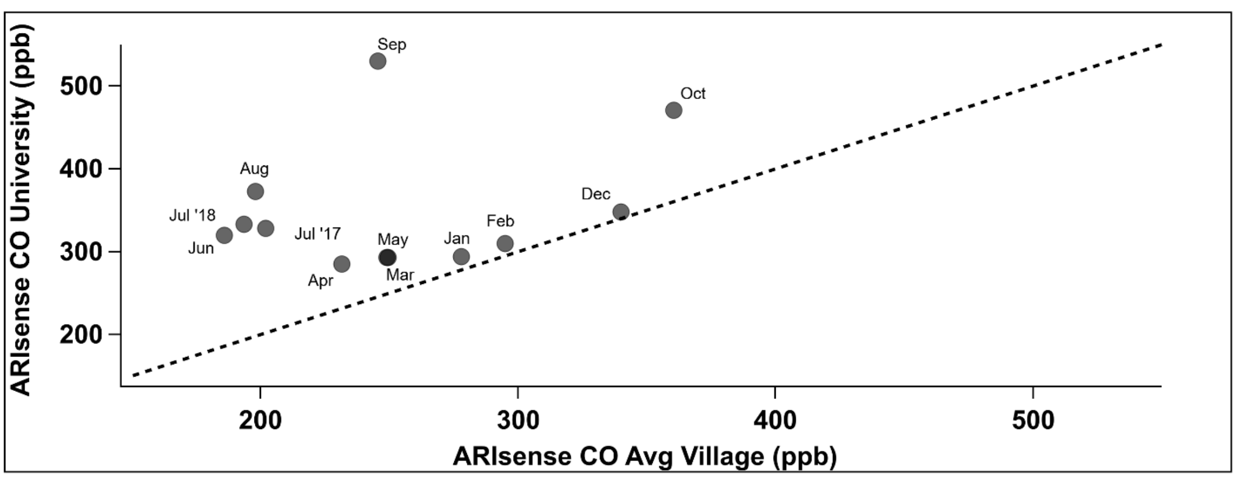

Figure S8: Scatter plot of University (y-axis) and Village Mean (average from Village 1 and 2) (x-axis) monthly mean CO concentration (calibrated with the kNN Hybrid model). A one-to-one line is shown as the dotted black line.

Table S2: NASA Goddard Earth Sciences Data and Information Services Center (GES-DISC) Interactive Online Visualization and Analysis Infrastructure information used to obtain MOPITT observations for two locations ("Village Mean" and "University") in Malawi.

	Data product	**Spatial Resolution**	**Temporal Resolution**	**Date Range**	**User Bounding Box ("Village Mean")**	**User Bounding Box ("University")**	**Data Bounding Box ("Village Mean")**	**Data Bounding Box ("University")**
MOPITT (satellite observation): The Measurement of Pollution in the Troposphere (MOPITT) sensor launched aboard Terra satellite	Time Series, Area-Averaged of Multispectral CO Surface Mixing Ratio (Daytime/Descending) monthly ()	1°	Monthly	2017-07-01 to 2018-07-31	35.5555°, -16.0451°, 35.5555°, -16.0451°	33.7744°, -14.18°, 33.7744°, -14.18°	36°, -16°, 36°, -16°	34°, -14°, 34°, -14°

Table S3: NASA Goddard Earth Sciences Data and Information Services Center (GES-DISC) Interactive Online Visualization and Analysis Infrastructure information used to obtain MERRA-2 observations for two locations ("Village Mean" and "University") in Malawi.

	Data product	**Spatial Resolution**	**Temporal Resolution**	**Date Range**	**User Bounding Box ("Village Mean")**	**User Bounding Box ("University")**	**Data Bounding Box ("Village Mean")**	**Data Bounding Box ("University")**
MERRA-2 (global atmospheric reanalysis): The Modern-Era Retrospective analysis for Research and Applications, Version 2 (MERRA-2); MERRA-2 Model M2TMNXCHM v5.12.4	Time Series, Area-Averaged of CO Surface Concentration (ENSEMBLE) monthly 0.5 x 0.625 deg. [MERRA-2 ()]	0.5° x 0.625°	Monthly	2017-07-01 to 2018-07-31	35.5555°, -16.0451°, 35.5555°, -16.0451°	33.7744°, -14.18°, 33.7744°, -14.18°	35.625°, -16°, 35.625°, -16°	33.75°, -14°, 33.75°, -14°

S7 Supporting figures from pre-collocation in North Carolina

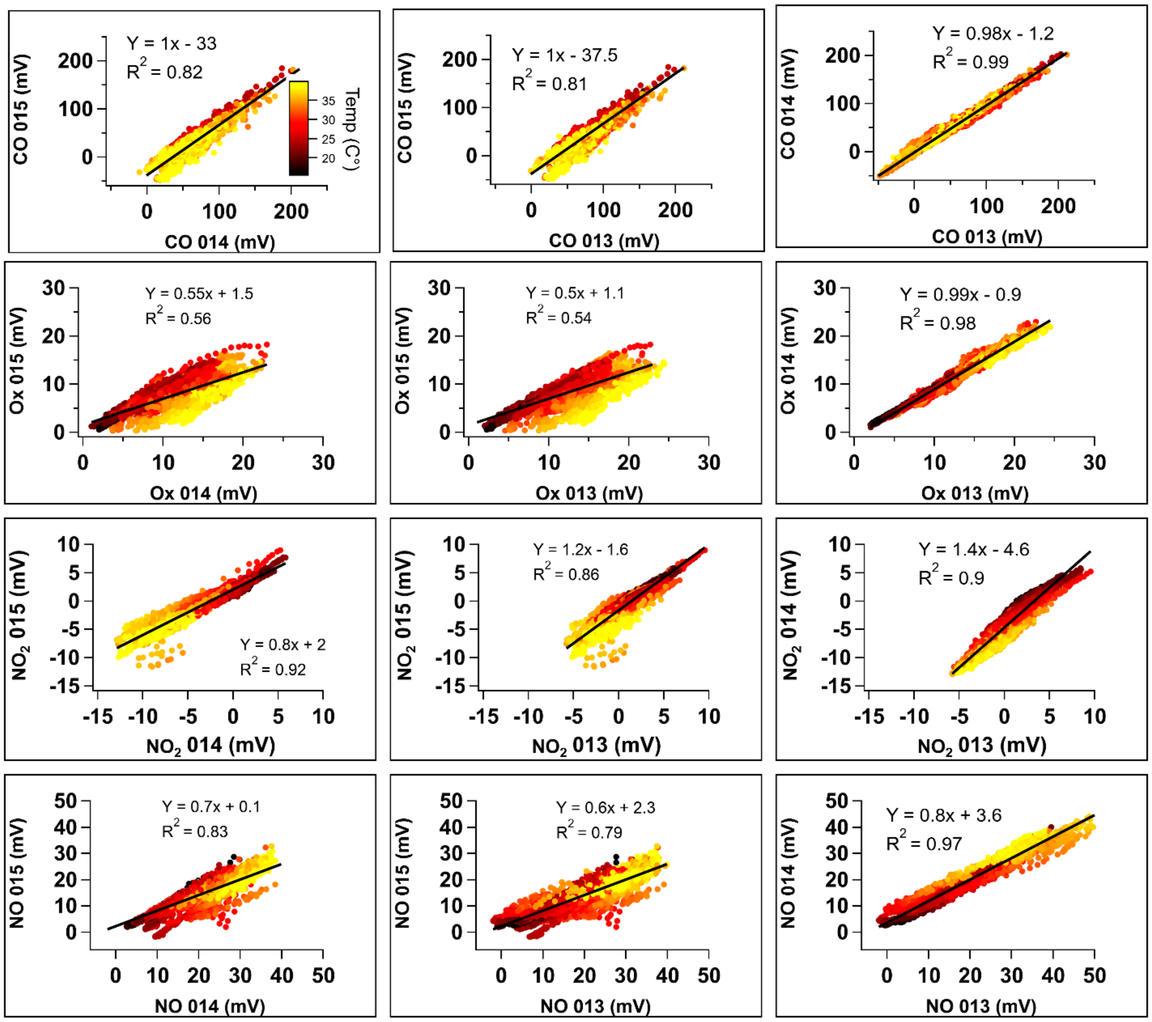

Figure S9: Scatter plots of raw differential voltage data from each gas sensor (rows) in each monitor pair (columns) during pre-collocation in NC. Linear fit coefficients (y = mx + b) and the Coefficient of Determination (R^2) are shown for each monitor-monitor gas sensor pair. Data points are colored by ambient temperature.

Table S4: ARI013 performance metrics for each gas sensor calibrated by the five modelling approaches used in this study*:* k-nearest neighbor (kNN) hybrid, random forest (RF) hybrid, high-dimensional model representation (HDMR), multi-linear regression (MLR), and quadratic regression (QR). Metrics were calculated only on a subset of the pre-colocation data that was not used to train the models. CO = carbon monoxide, NO = nitrogen oxide, NO_2 = nitrogen dioxide, O_x = oxidants. R^2 = Coefficient of Determination, cV = Coefficient of Variation, RMSE = Root Mean Square Error, Slope and Intercept are the fit regression coefficients from simple linear regression.

ARI013

	Slope	**Intercept**	**R^2**	**RMSE (ppb)**	**cV**
CO					
HDMR	0.66	102	0.63	65	0.30
MLR	0.66	102	0.63	65	0.30
kNN Hybrid	0.85	41	0.77	52	0.33
RF Hybrid	0.78	68	0.78	68	0.33
QR	0.75	76	0.72	58	0.34
NO					
HDMR	0.77	2	0.77	5	1.1
MLR	0.52	4	0.51	6	0.9
kNN Hybrid	0.87	1	0.87	3	1.2
RF Hybrid	0.80	2	0.86	7	1.1
NO_2					
HDMR	0.30	7	0.33	5	0.34
MLR	0.27	7	0.31	5	0.32
kNN Hybrid	0.68	2	0.58	4	0.52
RF Hybrid	0.54	4	0.60	5	0.43
O_x					
HDMR	0.94	1	0.94	3	0.53
MLR	0.92	2	0.92	3	0.52
kNN Hybrid	0.99	0	0.96	3	0.54
RF Hybrid	0.90	2	0.95	4	0.51

Table S5: ARI014 performance metrics for each gas sensor calibrated by the five modelling approaches used in this study: k-nearest neighbor (kNN) hybrid, random forest (RF) hybrid, high-dimensional model representation (HDMR), multi-linear regression (MLR), and quadratic regression (QR). Metrics were calculated only on a subset of the pre-colocation data that was not used to train the models. CO = carbon monoxide, NO = nitrogen oxide, NO^2 = nitrogen dioxide, O_x = oxidants. R^2 = Coefficient of Determination, cV = Coefficient of Variation, RMSE = Root Mean Square Error, Slope and Intercept are the fit regression coefficients from simple linear regression.

ARI014

	Slope	**Intercept**	**R^2**	**RMSE (ppb)**	**cV**
CO					
HDMR	0.72	84	0.70	58	0.31
MLR	0.72	84	0.70	58	0.31
kNN Hybrid	0.87	34	0.80	48	0.34
RF Hybrid	0.80	59	0.81	64	0.34
QR	0.79	64	0.76	62	0.34
NO					
HDMR	0.81	1	0.82	4	1.2
MLR	0.62	3	0.68	6	1.0
kNN Hybrid	0.92	0	0.93	3	1.2
RF Hybrid	0.82	1	0.88	7	1.1
NO2					
HDMR	0.33	6	0.37	4	0.35
MLR	0.27	7	0.32	5	0.33
kNN Hybrid	0.65	2	0.57	4	0.51
RF Hybrid	0.55	4	0.58	5	0.43
Ox					
HDMR	0.94	1	0.94	3	0.53
MLR	0.93	2	0.93	3	0.52
kNN Hybrid	0.98	0	0.96	3	0.54
RF Hybrid	0.89	3	0.95	4	0.51

Table S6: ARI015 performance metrics for each gas sensor calibrated by the five modelling approaches used in this study: k-nearest neighbor (kNN) hybrid, random forest (RF) hybrid, high-dimensional model representation (HDMR), multi-linear regression (MLR), and quadratic regression (QR). Metrics were calculated only on a subset of the pre-colocation data that was not used to train the models. CO = carbon monoxide, NO = nitrogen oxide, NO^2 = nitrogen dioxide, O_x = oxidants. R^2 = Coefficient of Determination, cV = Coefficient of Variation, RMSE = Root Mean Square Error, Slope and Intercept are the fit regression coefficients from simple linear regression.

ARI015

	Slope	**Intercept**	**R^2**	**RMSE (ppb)**	**cV**
CO					
HDMR	0.81	55	0.83	47	0.32
MLR	0.81	55	0.83	47	0.32
kNN Hybrid	0.91	23	0.88	40	0.34
RF Hybrid	0.83	51	0.93	68	0.33
QR	0.88	39	0.93	51	0.35
NO					
HDMR	0.88	1	0.89	3	1.10
MLR	0.80	1	0.81	4	1.04
kNN Hybrid	0.95	0	0.92	2	1.15
RF Hybrid	0.85	1	0.95	3	1.04
NO2					
HDMR	0.33	6	0.34	4	0.33
MLR	0.26	7	0.27	5	0.30
kNN Hybrid	0.71	2.	0.65	3	0.49
RF Hybrid	0.58	4	0.92	5	0.43
Ox					
HDMR	0.90	2	0.90	3	0.42
MLR	0.84	4	0.85	4	0.40
kNN Hybrid	0.98	0	0.95	2	0.44
RF Hybrid	0.84	4	0.99	7	0.37

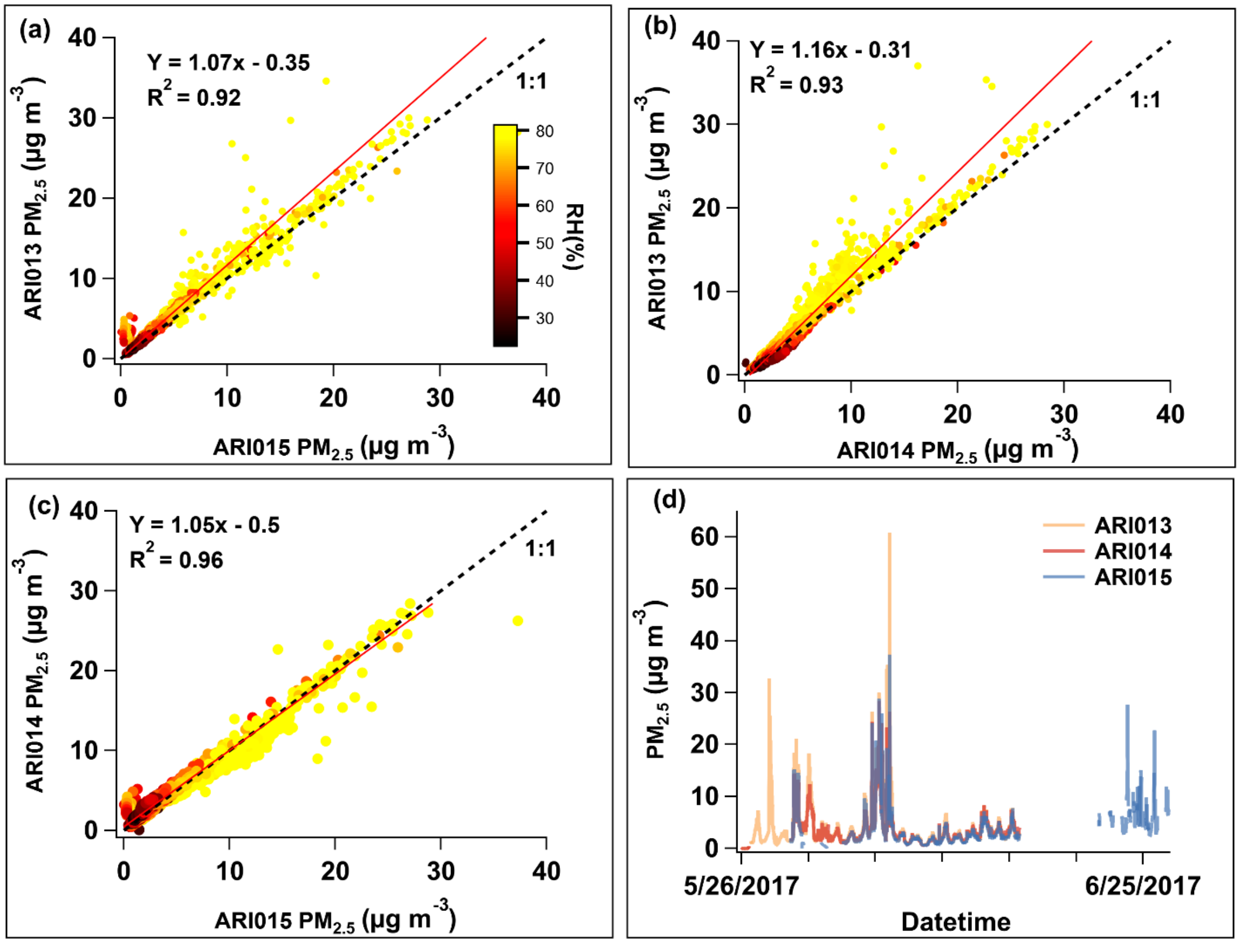

Figure S10: Intercomparison of (a) ARI013 and ARI015 $PM_{2.5}$ mass concentration measurements, (b) ARI013 and ARI015 $PM_{2.5}$ mass concentration measurements, and (c) ARI014 and ARI015 $PM_{2.5}$ mass concentration measurements during pre-collocation in NC. Point color indicates relative humidity conditions. Linear regression coefficients (y = mx + b), fit line (red line), and the Coefficient of Determination (R^2) are shown for each paired comparison; A one to one comparison line is shown as the dotted black line. The time series of $PM_{2.5}$ mass concentration measurements from ARI013, ARI014, and ARI015 (d) shows time alignment. Line color indicates ARISense unit number.

S8 Supporting figures from OPC-N2 collocation in Malawi

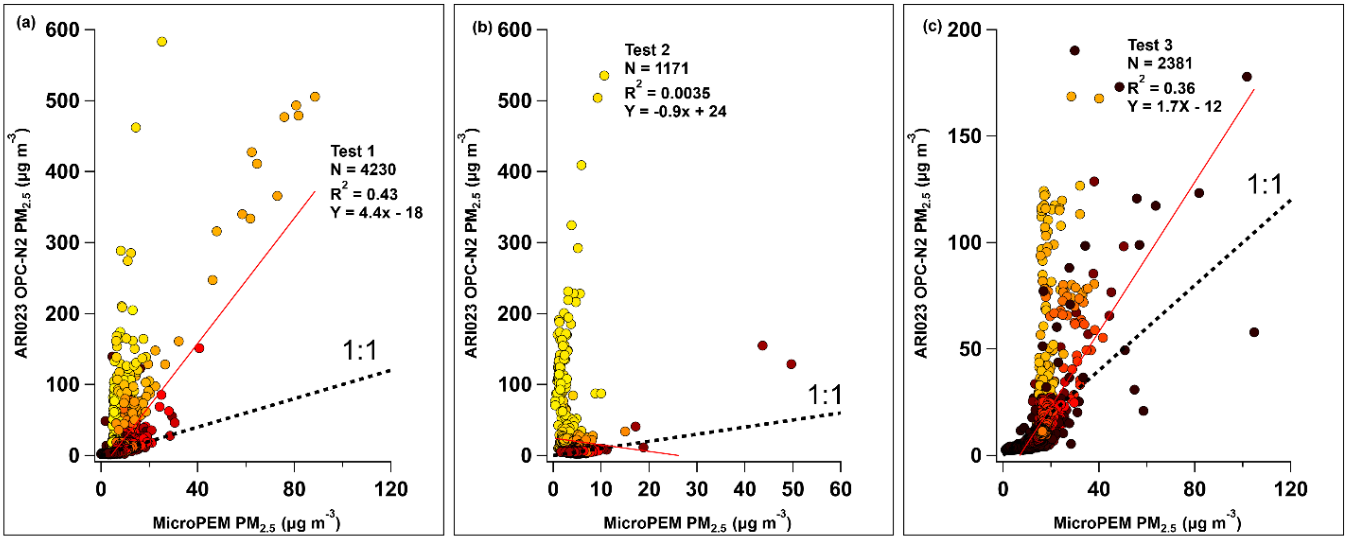

Figure S11: Scatter plots of uncorrected $PM_{2.5}$ mass concentration measurements from the Alphasense OPC-N2 sensor in ARI023 compared to measurements made by the mass-corrected MicroPEM nephelometer during collocation in Malawi for Test 1 (a), Test 2 (b), and Test 3 (c). Three tests were conducted over 130 hours. Point color indicates relative humidity conditions. Linear regression coefficients (y = mx + b), fit line (red line), and the Coefficient of Determination (R^2) are shown for each paired comparison; A one to one comparison line is shown as the dotted black line.

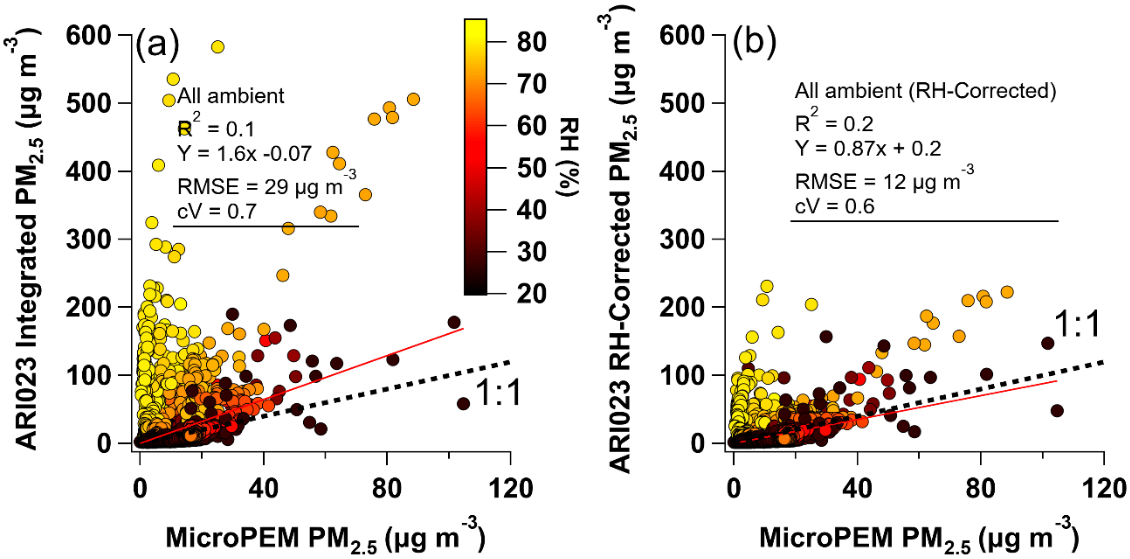

Figure S12: Scatter plots of (a) uncorrected and (b) RH-corrected $PM_{2.5}$ mass concentration measurements from the Alphasense OPC-N2 sensor in ARI023 compared to measurements made by the mass-corrected MicroPEM nephelometer during collocation in Malawi (1-min resolution). Point color indicates relative humidity conditions. Linear regression coefficients (y = mx + b), fit line (red line), the Coefficient of Determination (R^2), root mean square error (RMSE), and the coefficient of variation (cV) are shown for each paired comparison; A one to one comparison line is shown as the dotted black line.

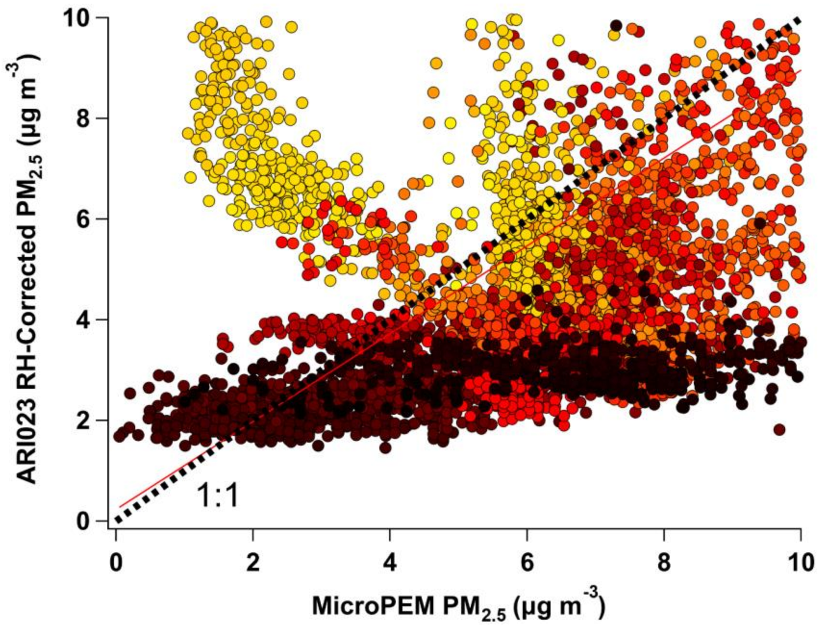

Figure S13: Zoom of Figure S12b.

Table S7: Metrics from the MicroPEM and uncorrected and RH-corrected OPC-N2 observations during collocation for three averaging intervals. R^2 = Coefficient of Determination, cV = Coefficient of Variation, RMSE = Root Mean Square Error, Slope and Intercept are the fit regression coefficients from simple linear regression.

Averaging Interval	Slope	Intercept	R^2	RMSE	cV
1 min uncorrected	1.6	0	0.1	29	2.1
1 hr uncorrected	0.7	9	0.03	22	1.5
24 hr uncorrected	-0.9	24	0.2	14	0.6
1 min RH Corrected	0.87	0	0.2	12	1.6
1 hr RH Corrected	0.43	4	0.06	9	1.1
24 hr RH Corrected	-0.27	11	0.1	6	0.4

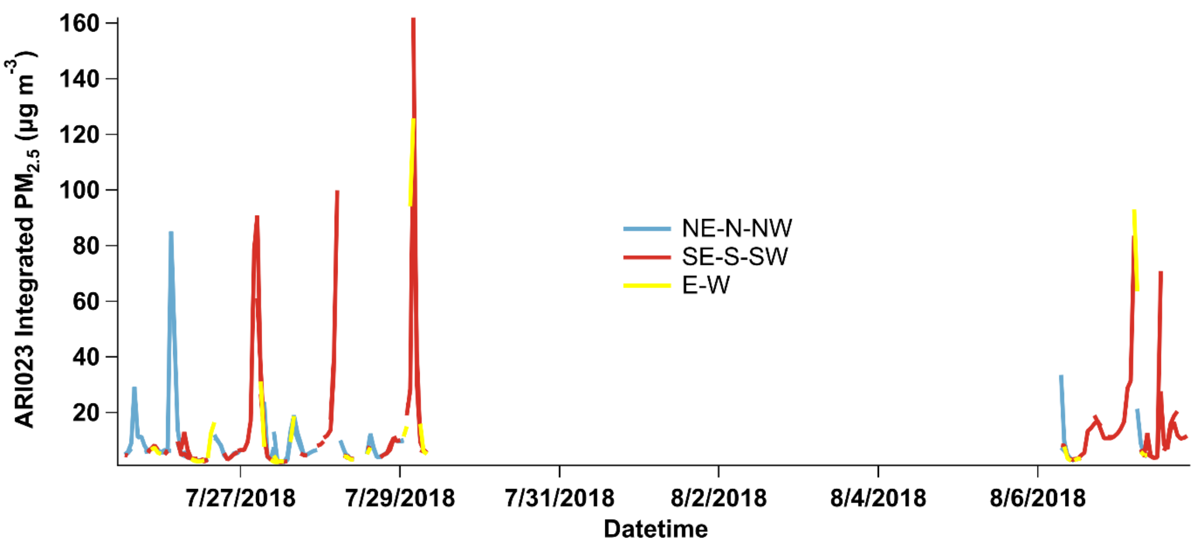

Figure S14: Times series of ARI023 uncorrected $PM_{2.5}$ concentration during colocation in Malawi. Data are colored by wind direction. Spikes in the time series are associated with widespread biomass cookstove use during the morning (5-7 AM). Cookstove activity was largely associated with southerly winds.

Table S8: Metrics for RH-corrected, 1-hr averaged data stratified by ambient concentration (as measured by MicroPEM), RH, and wind direction. R^2 = Coefficient of Determination, cV = Coefficient of Variation, RMSE = Root Mean Square Error, Slope and Intercept are the fit regression coefficients from simple linear regression.

Concentration (μg m^{-3})	**Slope**	**Intercept**	**R^2**	**RMSE**	**cV**
0-5	-2.2	14	0.06	11	1.5
5-10	1.3	-1	0.03	9	1.2
10-15	0.5	5	0.00	12	1.0
15-20	1.3	-11	0.02	10	0.77
20-105	0.38	3	0.17	19	0.68

RH (%)	**Slope**	**Intercept**	**R^2**	**RMSE**	**cV**
10 to 20	0.47	0	0.36	8	1.03
20 to 30	0.53	0	0.73	5	0.90
30 to 40	0.45	1	0.63	5	0.55
40 to 50	0.53	2	0.43	5	0.63
50 to 60	0.47	2	0.38	6	0.60
60 to 70	0.61	0	0.31	7	0.79
70 to 80	0.19	10	0.00	13	1.1
80 to 90	1.2	9	0.03	20	1.1

Wind direction	**Slope**	**Intercept**	**R^2**	**RMSE**	**cV**
N	0.41	3	0.13	5	0.83
NE	0.57	0	0.45	5	0.87
E	0.51	5	0.06	12	1.4
SE	0.41	5	0.04	11	1.4
S	0.31	5	0.04	10	1.1
SW	0.45	3	0.15	6	0.92
W	0.40	3	0.27	4	0.67
NW	0.62	1	0.34	4	0.84

Table S9*:* Performance metrics of $PM_{2.5}$ mass concentration measurements from the Alphasense OPC-N2 (ARI023) compared to the mass-corrected MicroPEM nephelometer during collocation in Malawi. The number of data points in all three scenarios are identical, but the assumed kappa value, applied as part of an RH-correction algorithm, is different. This RH-correction algorithm is based on the kappa value and 'shifting' the bin cut-offs (Di Antonio, et al. 2018). In this case, the assumed density is held constant, and the kappa value is changed. $\kappa = 0.6$ is the empirical value which achieved the best agreement between an OPC-N2 and reference data in the UK (Di Antonio (2018)). $\kappa = 1$ indicates an aerosol mixture with appreciable amounts of inorganics (theoretical value, based on Petters & Kreidenweis (2007)). $\kappa = 0.15$ was reported to be the continental average value for Africa, based on Pringle et al, 2010 and Pope at. al, 2018 (modelled and observed). Data are 60-min averaged. R^2 = Coefficient of Determination, cV = Coefficient of Variation, RMSE = Root Mean Square Error.

Kappa	**Slope**	**Intercept**	**R^2**	**RMSE**	**cV**
0.15	0.59	5	0.05	14	1.3
0.6	0.41	4	0.07	9	1.06
1	0.32	4	0.08	8	0.97

Table S10: Performance metrics of PM2.5 mass concentration measurements from the Alphasense OPC-N2 (ARI023) compared to the mass-corrected MicroPEM nephelometer during collocation in Malawi. The number of data points in all scenarios are identical, but the assumed kappa value, applied as part of an RH-correction algorithm, and the assumed density is different in each. This RH-correction algorithm is based on the kappa value and 'shifting' the bin cut-offs (Di Antonio, et al. 2018). Species data (κ and density) based on Hagan & Kroll (2020) & Petters & Kreidenweis (2007). Data are 60-min averaged. R^2 = Coefficient of Determination, cV = Coefficient of Variation, RMSE = Root Mean Square Error.

Aerosol type	**Kappa**	**Density (g cm^{-3})**	**Slope**	**Intercept**	**R^2**	**RMSE**	**cV**
Ammonium Nitrate	0.67	1.72	0.42	4	0.08	9	1.04
Dust	0.03	2.6	0.58	6	0.04	32	1.43
Wildfire	0.1	1.58	1.02	12	0.03	15	1.35
Background	0.25	1.45	0.35	6	0.03	12	1.32

S9 Supporting figures of ARISense performance during Malawi deployments

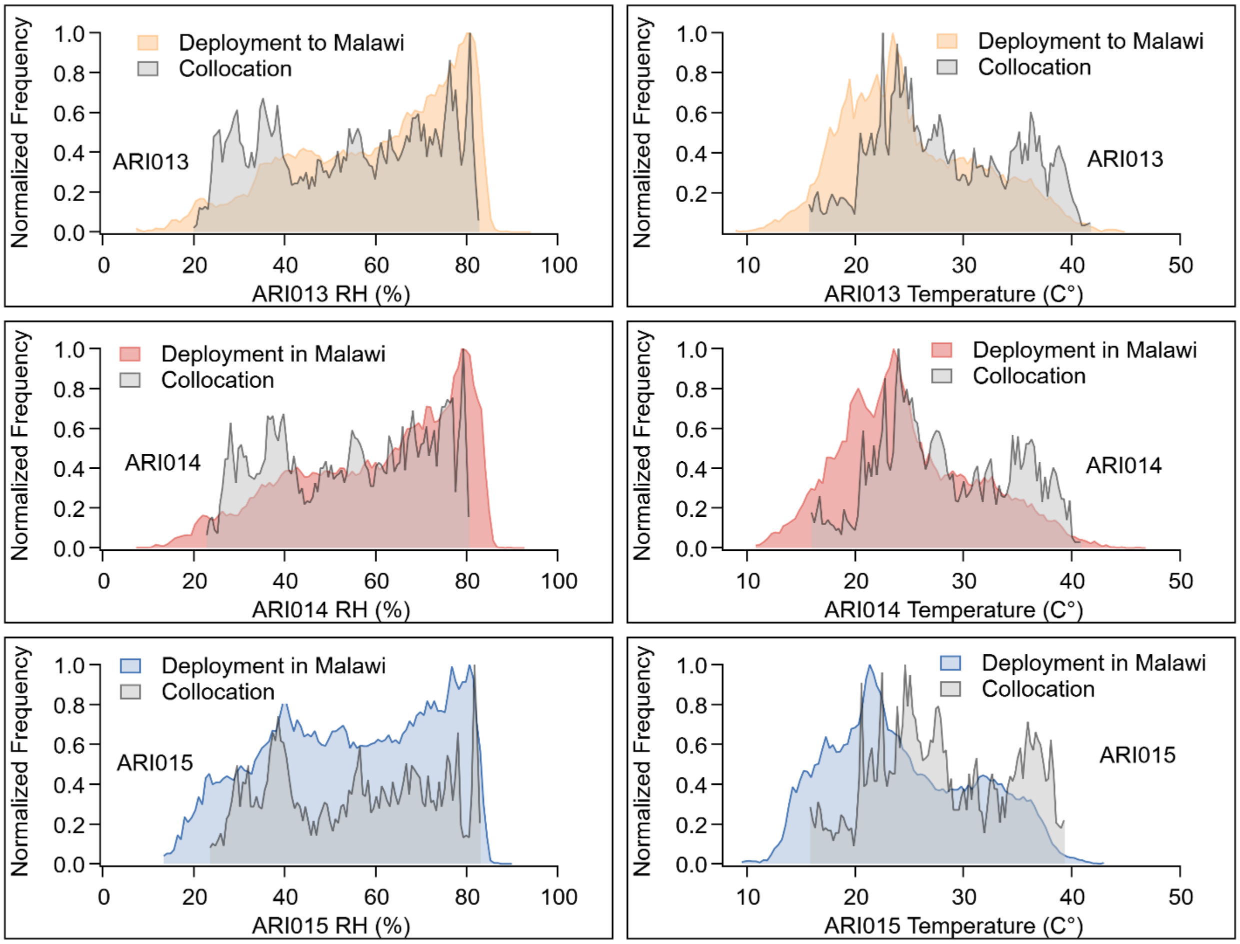

Figure S15: Relative humidity (RH) (left) and temperature (right) normalized frequency histograms for the NC pre-colocation (grey) and Malawi deployment (color) environments for all three ARISense monitors. ARI013 was deployed to the Village 2 site, ARI014 to the Village 1 site, and ARI015 to the University site. Histogram color indicates ARISense unit number in deployment environment.

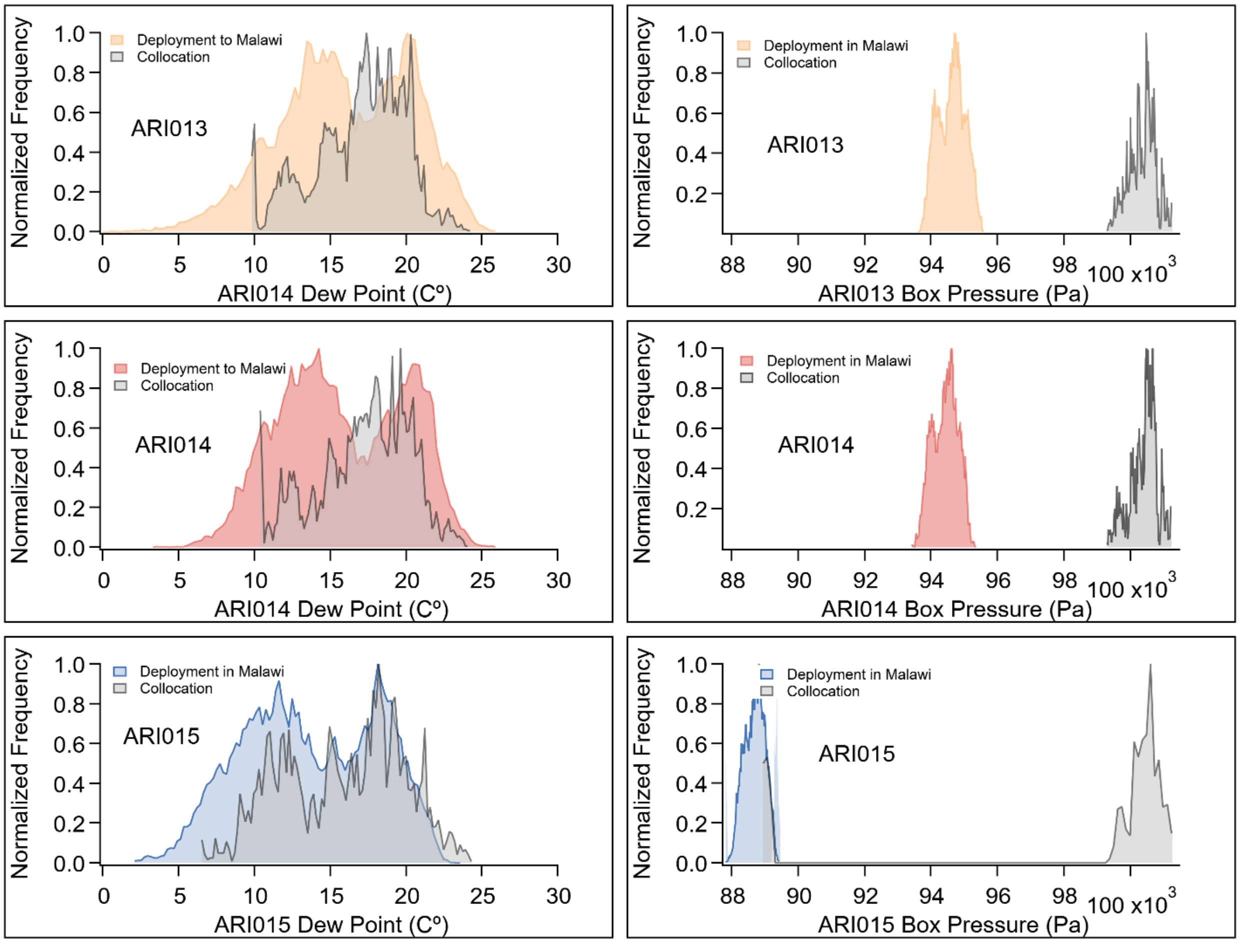

Figure S16: Dew point (left) and pressure (right) normalized frequency histograms for the collocation (grey) and deployment (color) environments for all three ARISense monitors. ARI013 was deployed to the Village 2 site, ARI014 to the Village 1 site, and ARI015 to the University site. Histogram color indicates ARISense unit number in deployment environment.

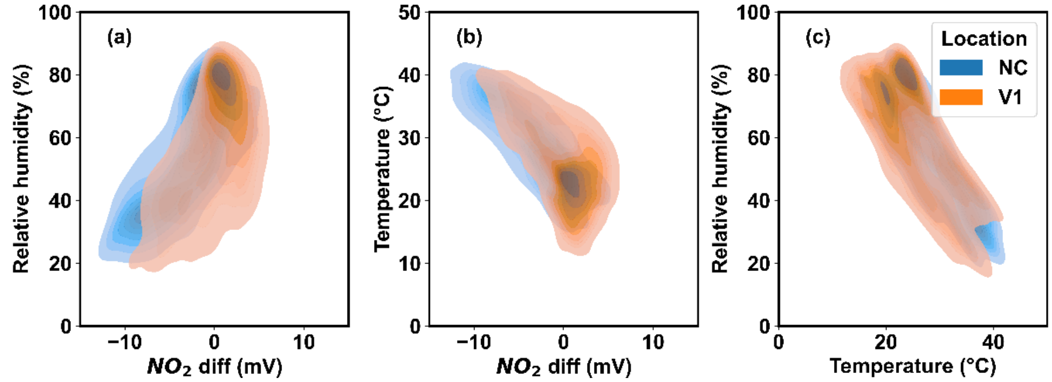

Figure S17: Bivariate distributions of ARI014 NO_2 differential voltage, RH, and T data collected during collocation (blue) and deployment (orange) made using kernel density estimation. NC = North Carolina, V1 = Village 1. Density is reflected in the color scheme; Darker colors indicate more data points in that region.

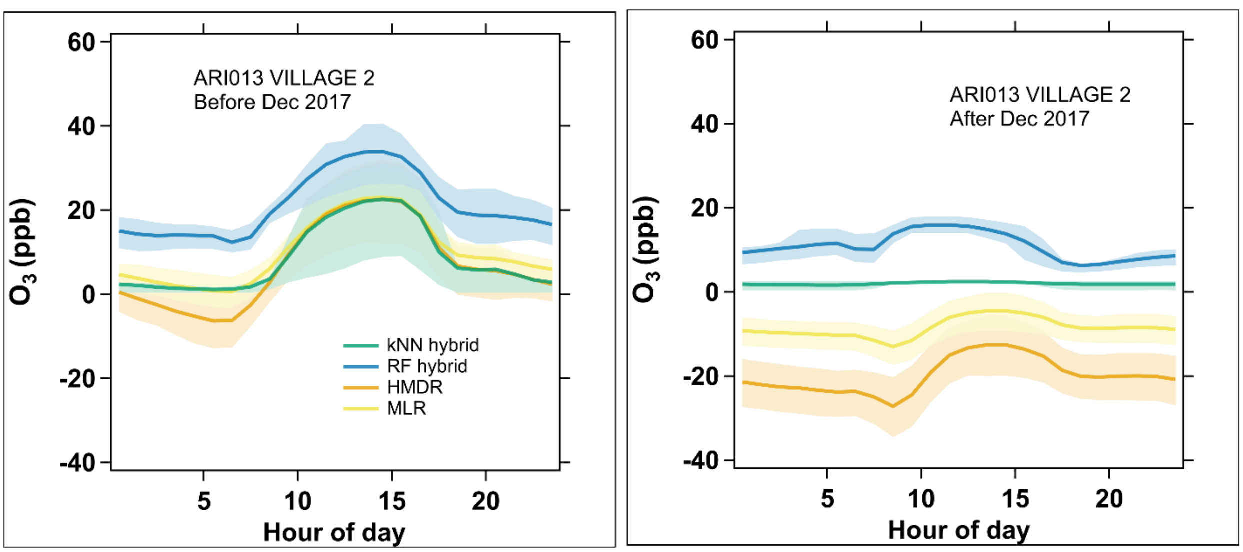

Figure S18*:* Diurnal trends of calibrated ozone data from ARI013 (Village 2 site) before Dec 2017 (left) and after Dec 2018 (right). Thick line indicates hourly mean, shaded region indicates interquartile range. Midnight is the zero hour. Line color indicates model type. Hours are in local time.

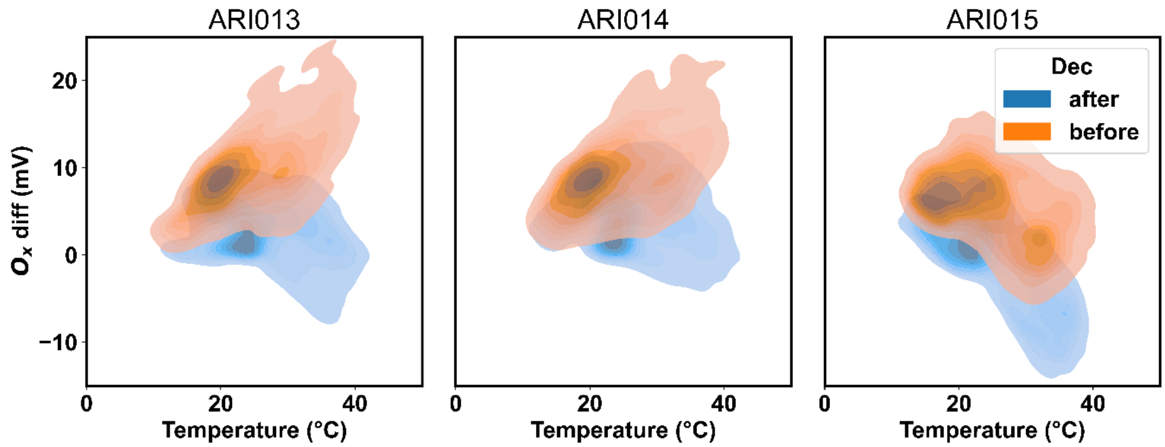

Figure S19: Bivariate distributions of O_x voltage and temperature data collected during the first half of deployment (July-November 2017 - orange) and in the second half of deployment (December 2017-July 2018 – blue) for each ARISense monitor using kernel density estimation. Density is reflected in the color scheme; Darker colors indicate more data points in that region.

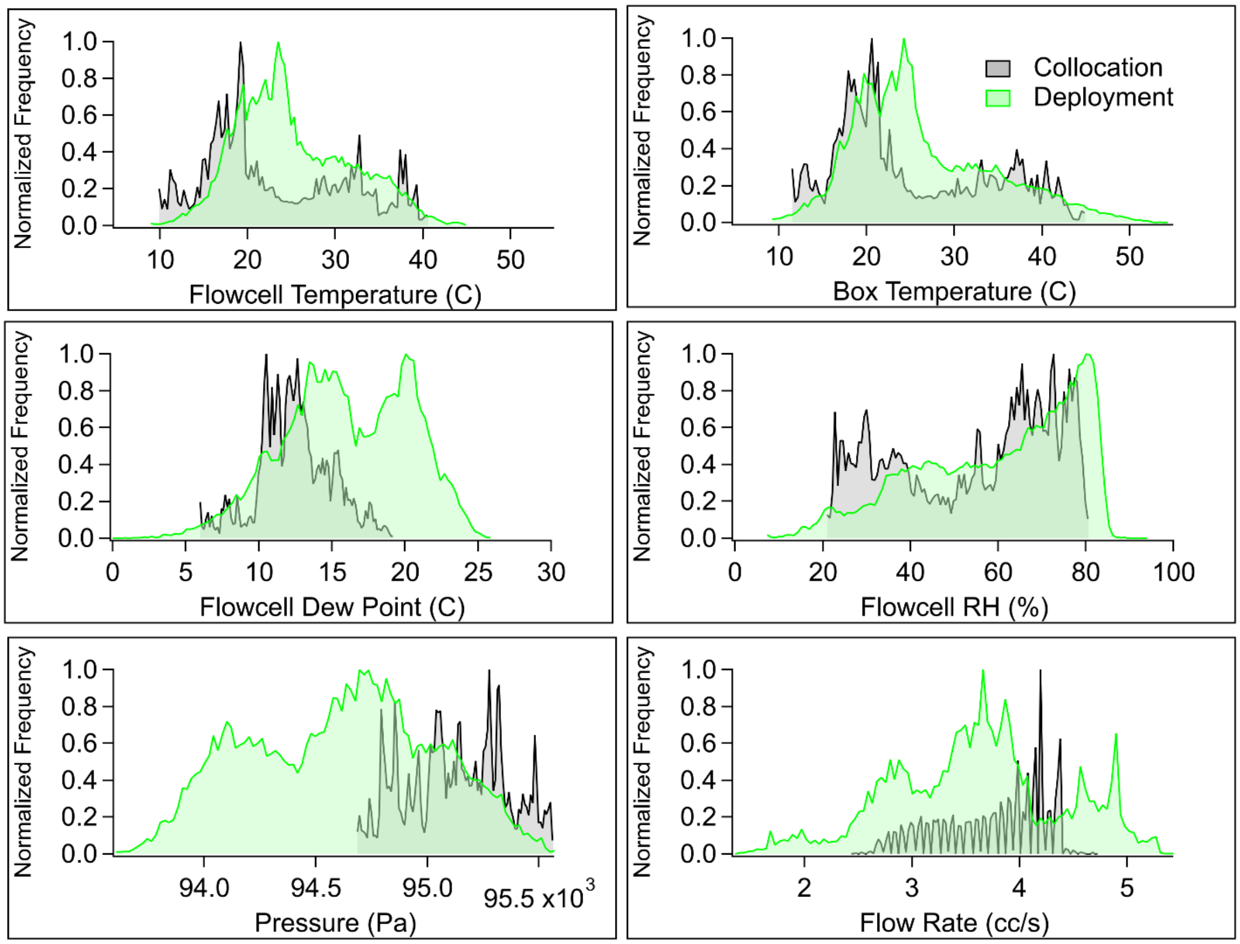

Figure S20: ARISense temperature (flow cell and box), dew point, relative humidity, pressure and flow rate normalized frequency histograms for the 130-hour OPC-N2 collocation (ARI023 in grey) in Malawi and the 1-year deployment in Malawi (ARI013 in green).

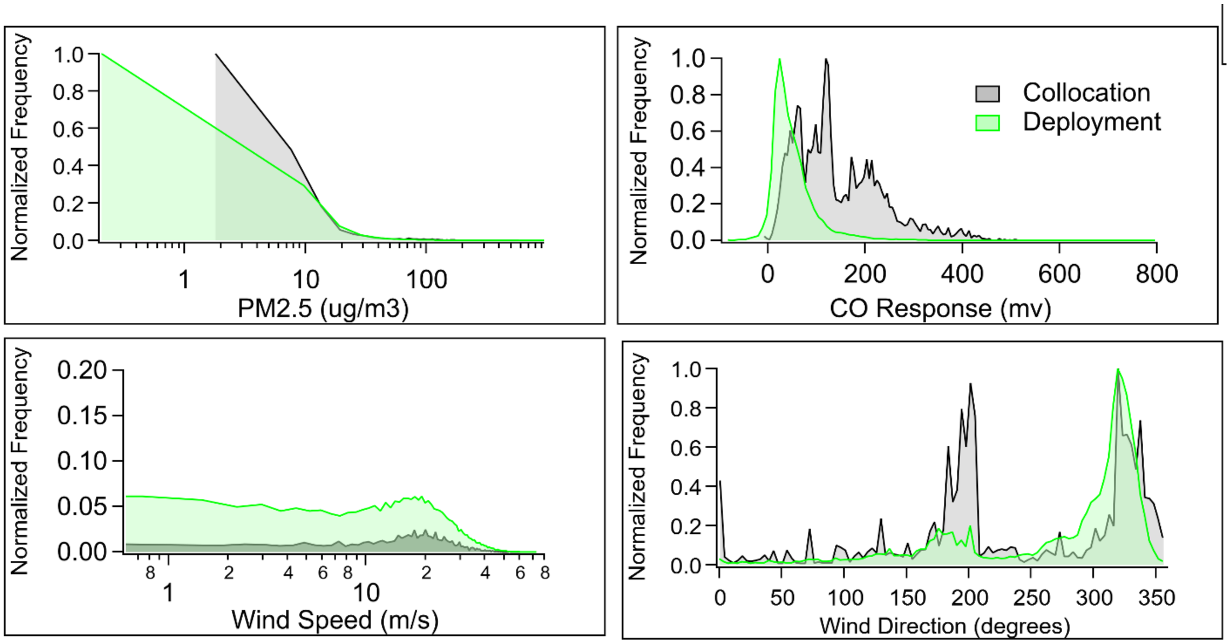

Figure S21: ARISense CO differential voltage, $PM_{2.5}$ mass concentration, wind speed, and wind direction normalized frequency histograms for the 130-hour OPC-N2 collocation (ARI023 in grey) in Malawi and the 1-year deployment in Malawi (ARI013 in green).

S10 Supporting figures of ARISense performance over time

(a)

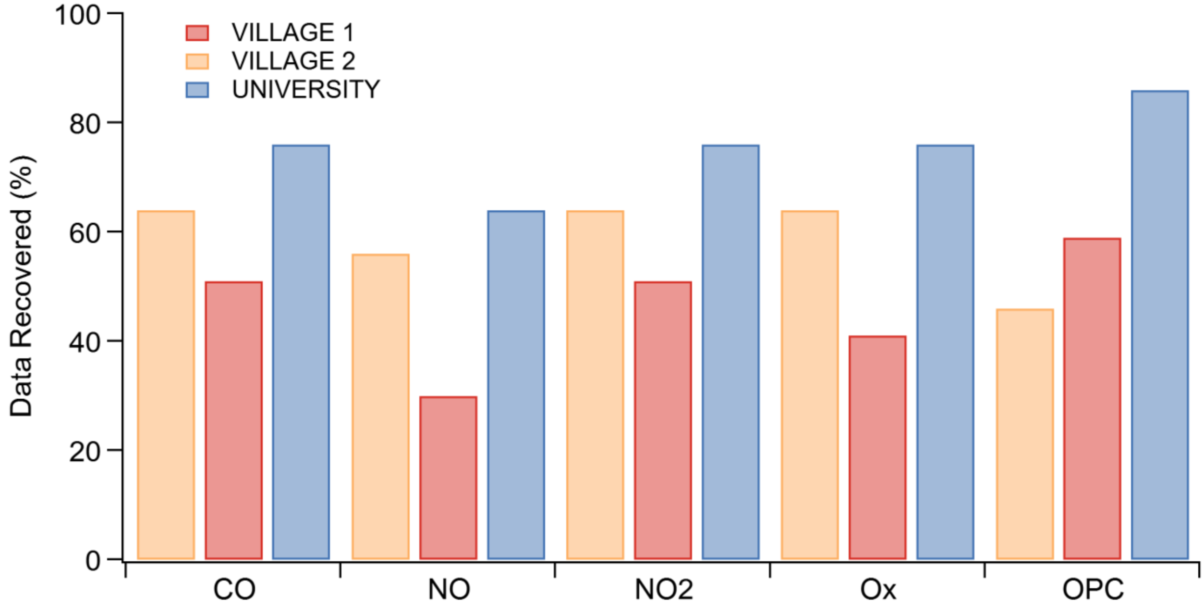

(b)

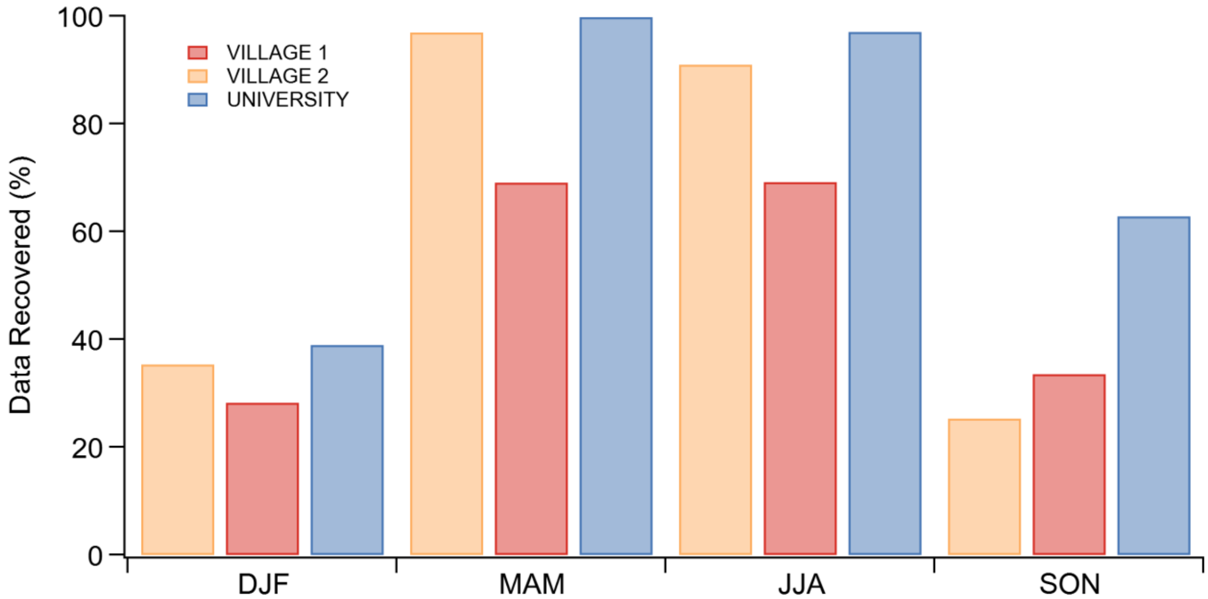

Figure S22: Data recovery rate (%) for the 1-year deployment for each ARISense monitor at their respective sites; (a) shows data recovery by sensor type where CO = carbon monoxide, NO = nitric oxide, NO2 = nitrogen dioxide, Ox = oxidants, and OPC = Optical Particle Counter, (b) shows data recovery by season (using the CO differential voltage sensor data recovery rate) where DJF = December-January-February, MAM = March-April-May, JJA = June-July-August, and SON = September-October-November.

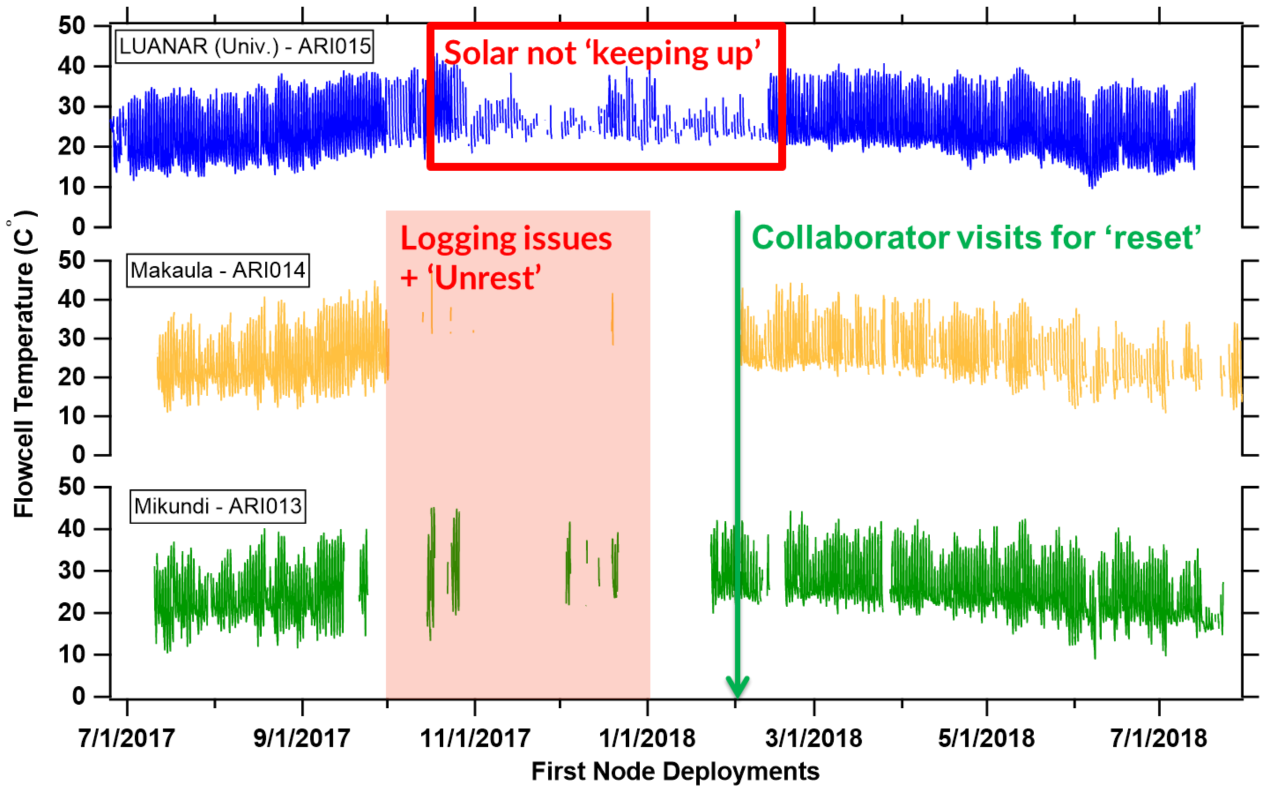

Figure S23: Timeseries of temperature data from ARI015 (top), ARI014 (middle), and ARI013 (bottom) from the full 1-year pilot deployment in Malawi. LUANAR = University, Makaula = Village 1, and Mikundi = Village 2. Gaps in the timeseries indicate periods when the ARISense were not collecting data. Text labels indicate the causes of data loss: 'solar not keeping up' refers to insufficient solar power in the winter months; 'logging issues and unrest' refer to the combination of corrupted USB devices which failed to log data, and a period of social unrest in the southern region of the country which created unsafe conditions for our assistant to visit the monitors; 'collaborator visits for reset' indicate when a collaborator visited the village locations to replace the USB devices and update the firmware.

S11 Comparison of first and last month of deployment data

Histograms of T and RH from July 2017 and July 2018 suggest the range in conditions was the same for both years, particularly for temperature (Fig. S24). However, for the Village 2 site, the average and maximum RH were higher by 10-15% in July 2018 compared to July 2017. Further, the mean temperature was 2° cooler in 2018. Conversely, at the University site in 2018, the average RH was 6% higher, while the minimum RH was 5% lower, compared to 2017 suggesting more variable environmental conditions in the second year. However, for the Village 1 and University sites, the mean temperatures were identical for both years.

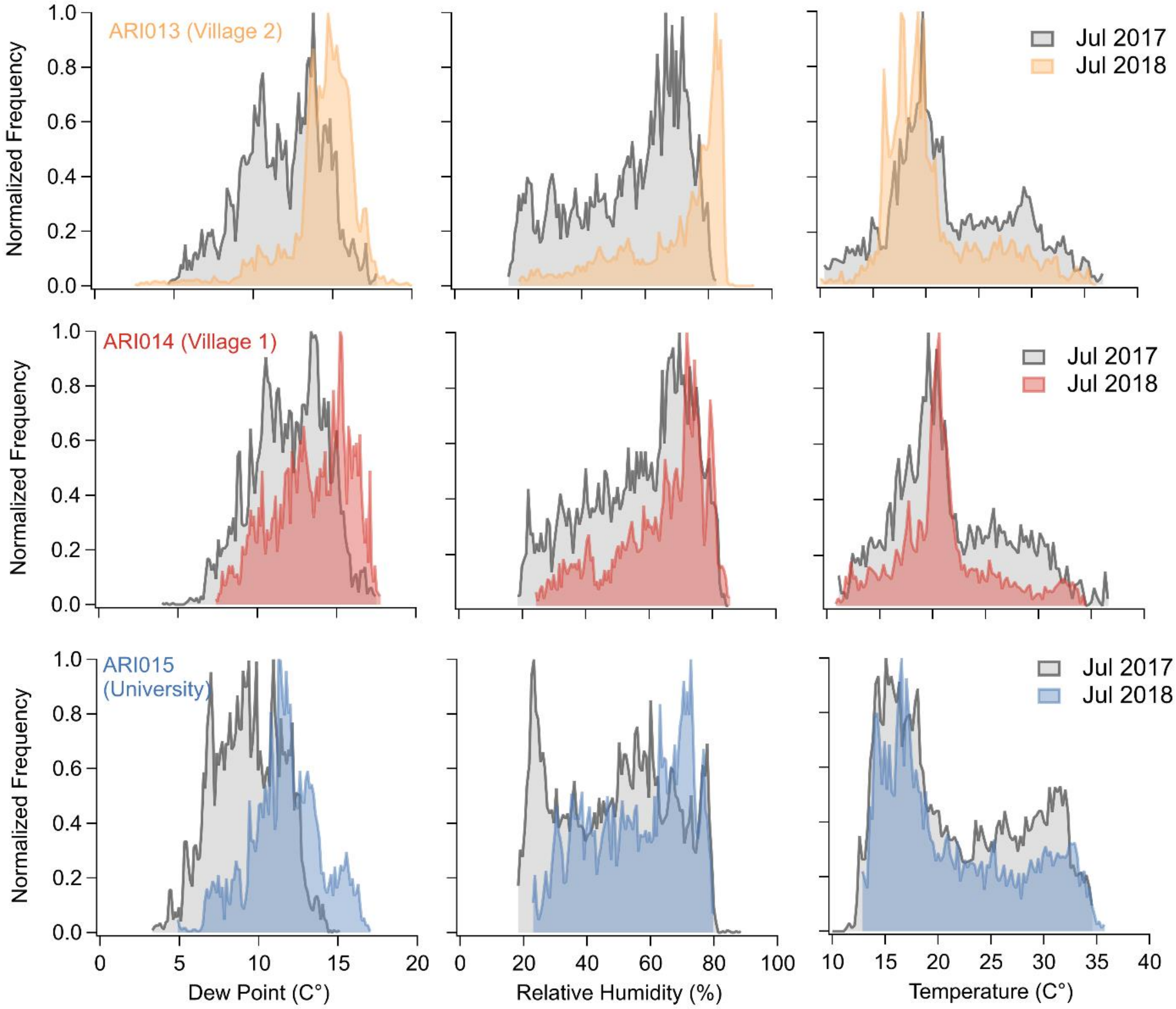

Figure S24: Dew point (left), RH (center), and temperature (right) normalized frequency histograms from the first month of deployment (grey) and last month of deployment (colored) for ARI013, ARI014, and ARI015 at their respective deployment sites.

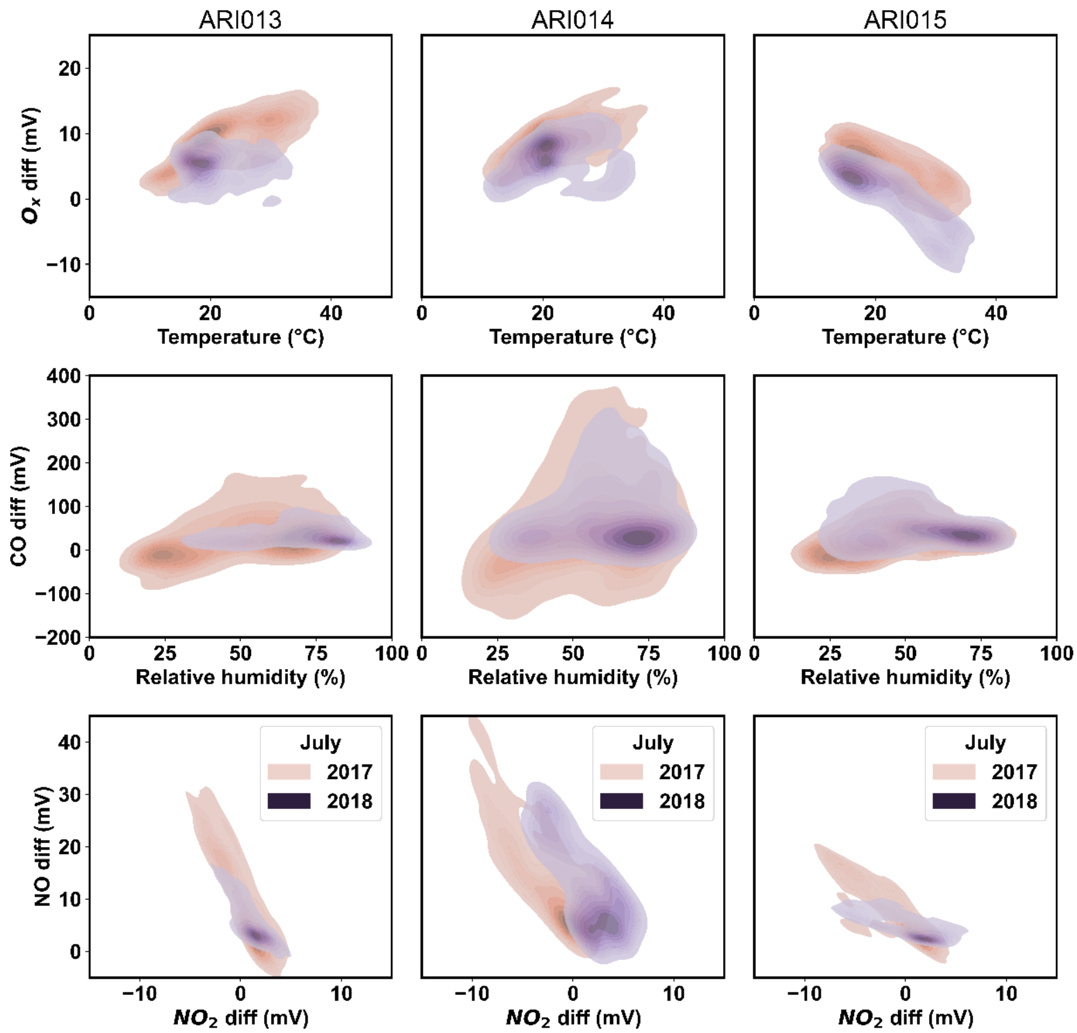

Figure S25: Bivariate distributions of data collected during the first month of deployment (July 2017) and data collected one year later in the last month of deployment (July 2018) for each ARISense monitor using kernel density estimation. Density is reflected in the color scheme; Darker colors indicate more data points in that region.

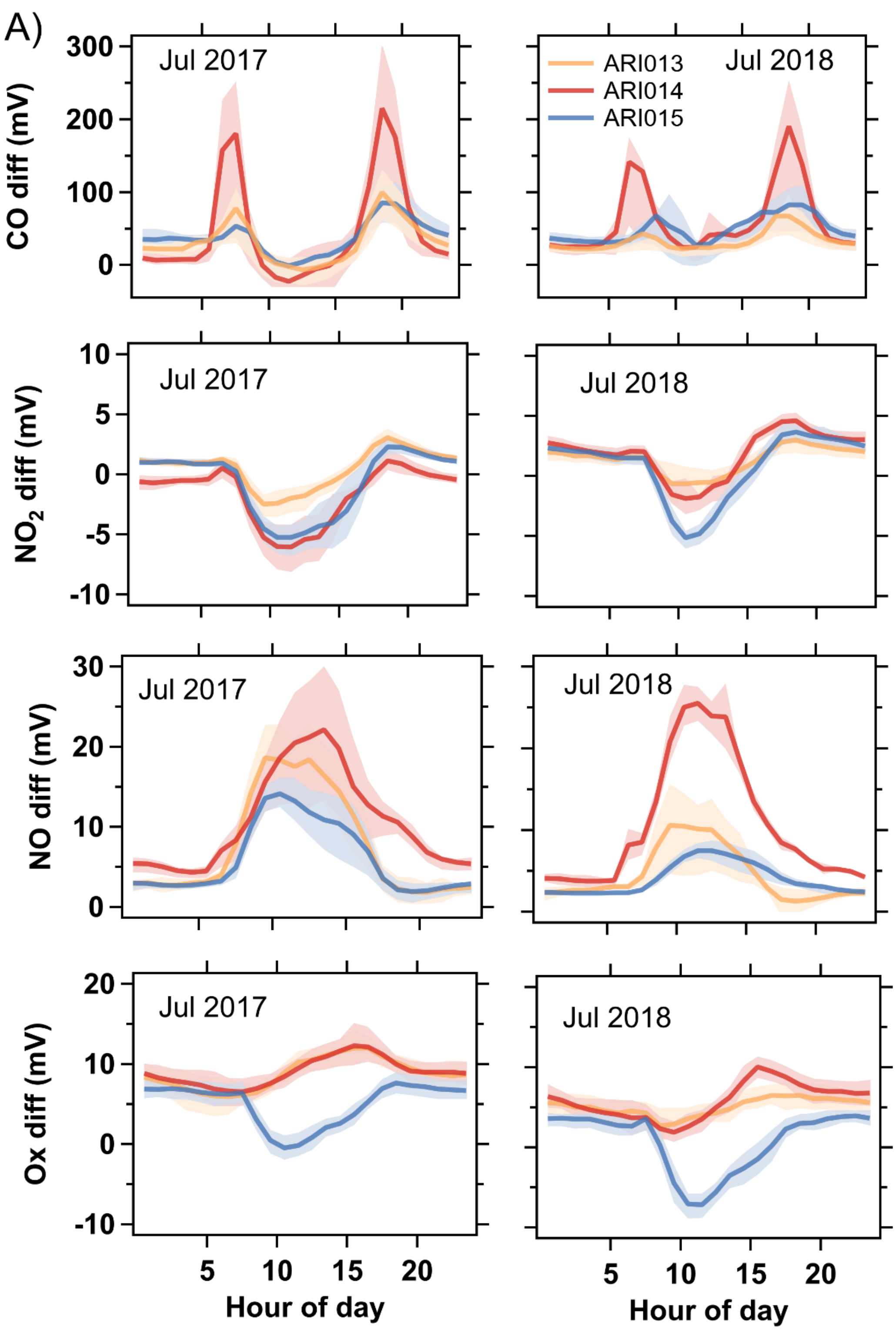

Figure S26: Diurnal trends of raw, uncalibrated voltage readings from July 2017 (left) and July 2018 (right), for each ARISense at each respective monitoring location. Thick line indicates hourly mean, shaded region indicates interquartile range. Midnight is the zero hour. Line color indicates sensor.

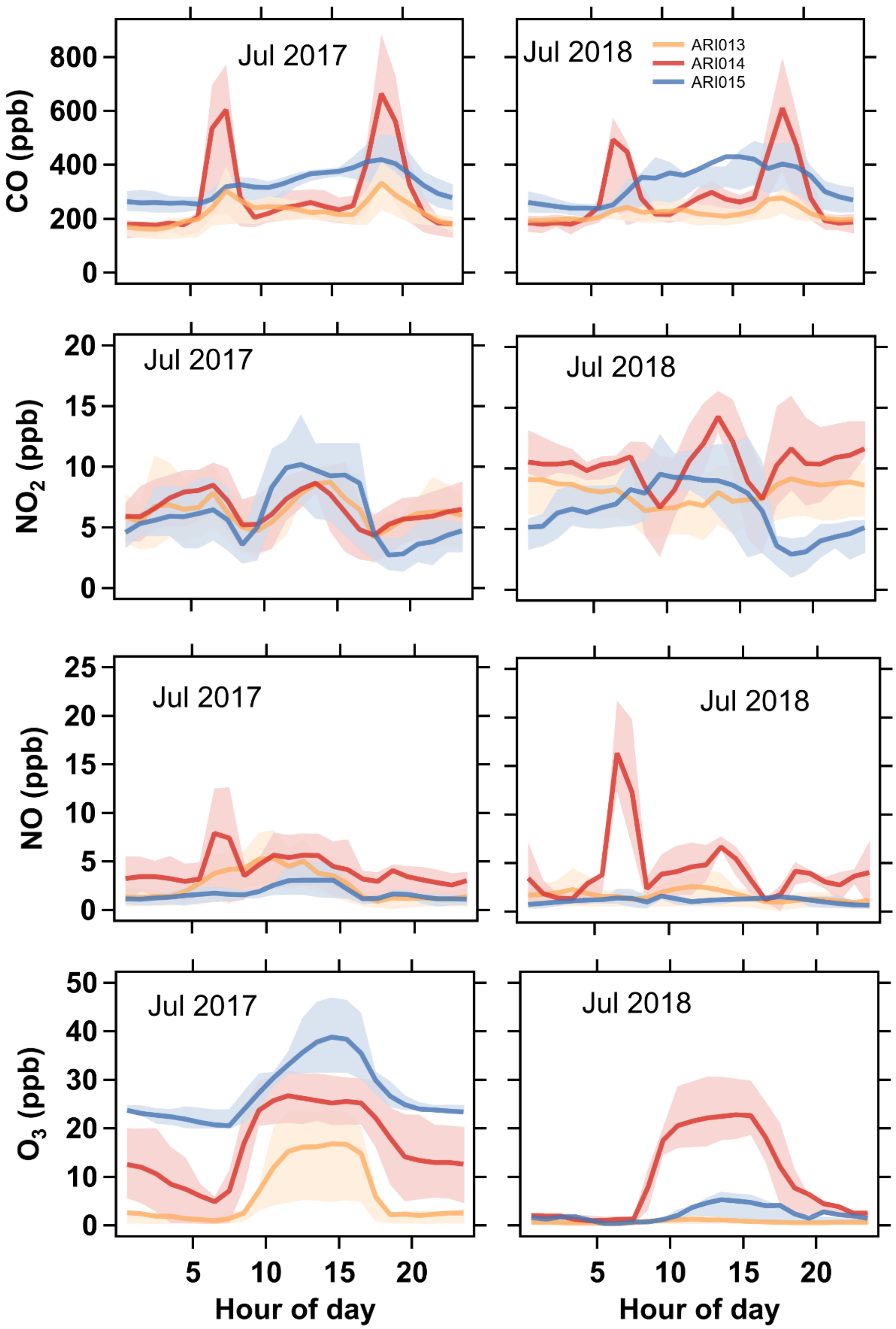

Figure S27: Diurnal trends of kNN-hybrid model calibrated concentration readings from July 2017 (left) and July 2018 (right), for each ARISense at each respective monitoring location. Thick line indicates hourly mean, shaded region indicates interquartile range. Midnight is the zero hour. Line color indicates sensor.

S12 Supporting figures for post-deployment collocation in North Carolina

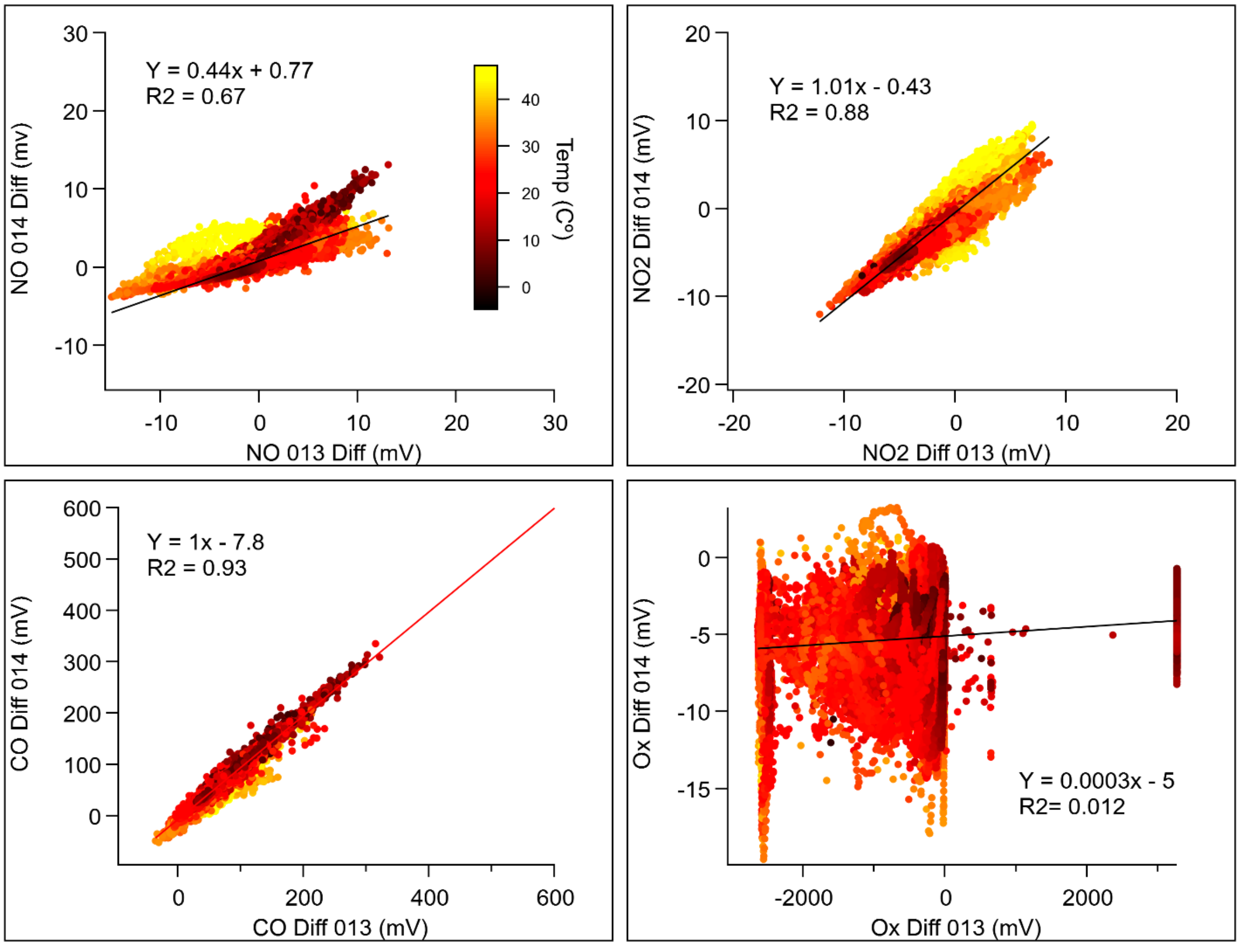

Figure S28: Scatter plots of raw differential voltage data from each gas sensor in ARI014 (y-axis) and ARI013 (x-axis) measured during post-collocation in North Carolina. Linear fit coefficients and the coefficient of determination (R^2) are shown for each monitor-monitor gas sensor pair. Data points are colored by ambient temperature.

Table S11: ARI013 post-collocation performance metrics for each gas sensor calibrated by the five modelling approaches used in this study: k-nearest neighbor (kNN) hybrid, random forest (RF) hybrid, high-dimensional model representation (HDMR), multi-linear regression (MLR), and quadratic regression (QR). CO = carbon monoxide, NO = nitrogen oxide, NO_2 = nitrogen dioxide, Ox = oxidants. R^2 = Coefficient of Determination, cV = Coefficient of Variation, RMSE = Root Mean Square Error, Slope and Intercept are the fit regression coefficients from simple linear regression.

ARI013

	Slope	**Intercept**	**R^2**	**RMSE (ppb)**	**cV**
CO					
HDMR	0.54	63	0.52	128	0.48
MLR	0.54	63	0.52	128	0.48
kNN Hybrid	0.54	99	0.66	98	0.37
RF Hybrid	0.5	104	0.72	99	0.34
QR	0.80	-57	0.45	179	0.93
NO					
HDMR	0.23	-19	0.04	36.10	-1.18
MLR	0.16	0.21	0.07	18.70	4.82
kNN Hybrid	0.012	0.88	0.03	19.60	1.21
RF Hybrid	0.04	5.36	0.02	16.70	0.818
NO2					
HDMR	-0.1	1.1	0.02	13.20	18.19
MLR	-0.2	-0.8	0.06	16.50	-2.17
kNN Hybrid	-0.04	5.1	0.01	9.60	0.654
RF Hybrid	-0.002	6.5	0.00	8.00	0.376
Ox					
HDMR	0.13	-21.6	0.00	86.27	-8.11
MLR	0.05	9.67	0.00	49.80	2.9
kNN Hybrid	0.096	13.11	0.00	44.70	2.26
RF Hybrid	-0.58	72.9	0.00	454.77	7.126

Table S12: ARI014 post-collocation performance metrics for each gas sensor calibrated by the five modelling approaches used in this study: k-nearest neighbor (kNN) hybrid, random forest (RF) hybrid, high-dimensional model representation (HDMR), multi-linear regression (MLR), and quadratic regression (QR). CO = carbon monoxide, NO = nitrogen oxide, NO_2 = nitrogen dioxide, Ox = oxidants. R^2 = Coefficient of Determination, cV = Coefficient of Variation, RMSE = Root Mean Square Error, Slope and Intercept are the fit regression coefficients from simple linear regression.

ARI014

	Slope	**Intercept**	**R^2**	**RMSE (ppb)**	**cV**
CO					
HDMR	0.59	37	0.59	131	0.52
MLR	0.59	37	0.59	131	0.52
kNN Hybrid	0.57	80	0.70	100	0.39
RF Hybrid	0.52	87	0.72	103	0.36
QR	0.79	-62	0.498	174	0.90
NO					
HDMR	0.27	-15	0.09	30	-1.1
MLR	0.22	0	0.06	21	8.4
kNN Hybrid	0.00	01	0.01	20	0.91
RF Hybrid	0.05	7	0.02	17	0.81
NO2					
HDMR	-0.19	8	0.03	12	1.3
MLR	-0.35	3	0.07	17	-53
kNN Hybrid	-0.1	7	0.02	10	0.92
RF Hybrid	0.06	8	0.01	8	0.45
Ox					
HDMR	-1.4	-31	0.21	97	-0.58
MLR	0.59	-15	0.23	57	-0.54
kNN Hybrid	0.46	1	0.33	16	1.03
RF Hybrid	0.00	9	0.00	20	0.42

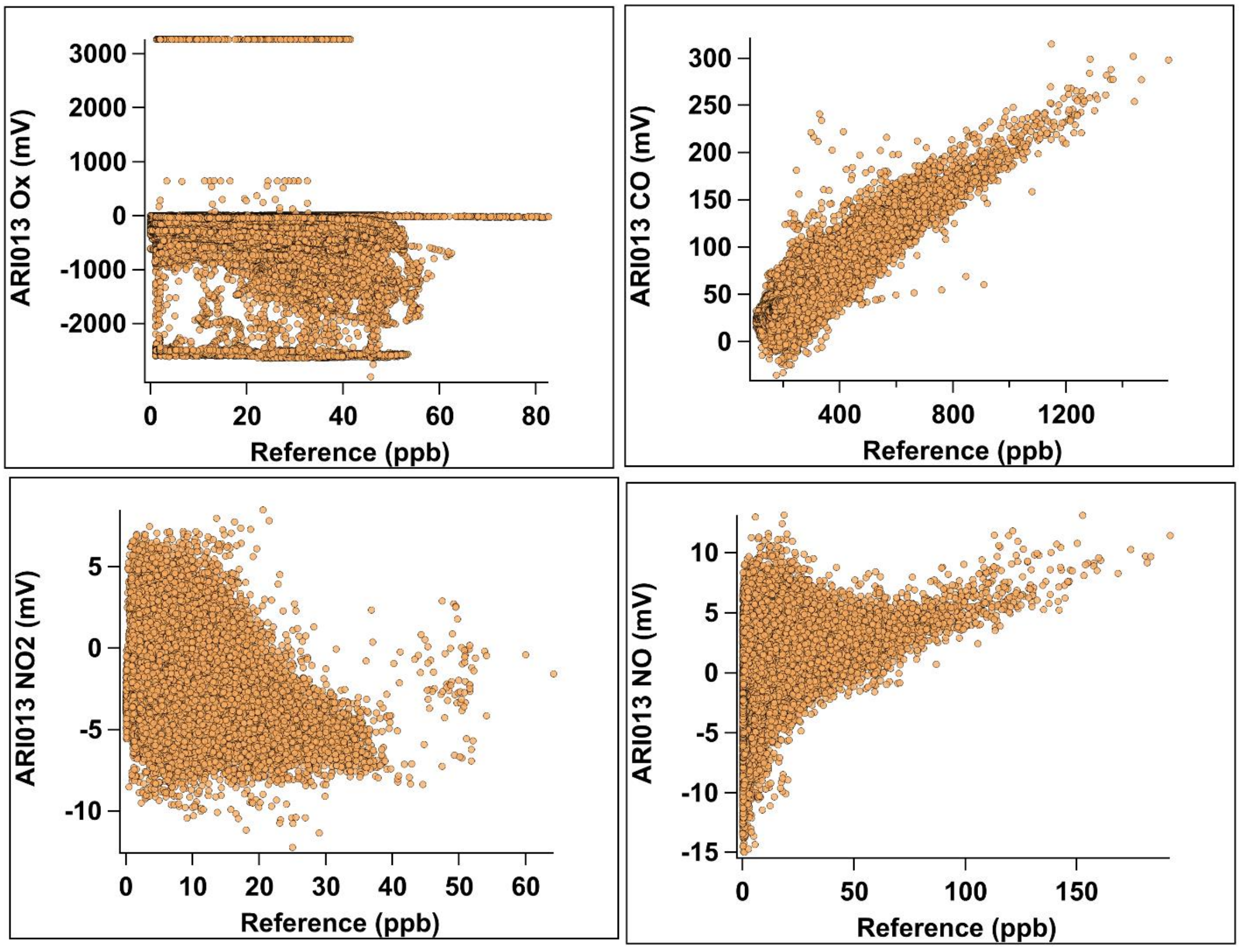

Figure S29: Scatter plots of raw differential voltage data from each gas sensor in ARI013 (y-axis) compared to reference data (x-axis) during post-deployment collocation in North Carolina.

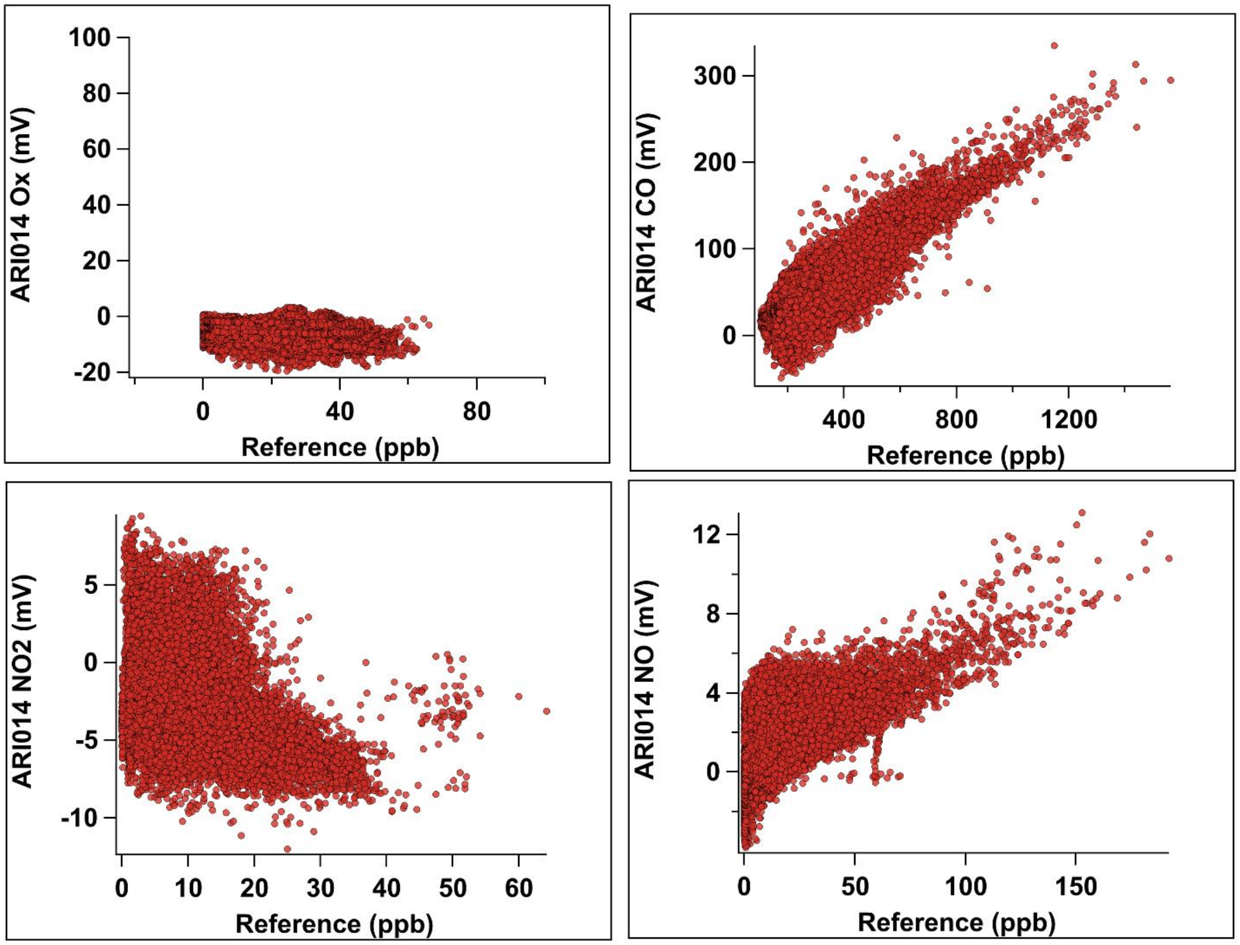

Figure S30: Scatter plots of raw differential voltage data from each gas sensor in ARI014 (y-axis) compared to reference data (x-axis) during post-deployment collocation in North Carolina.

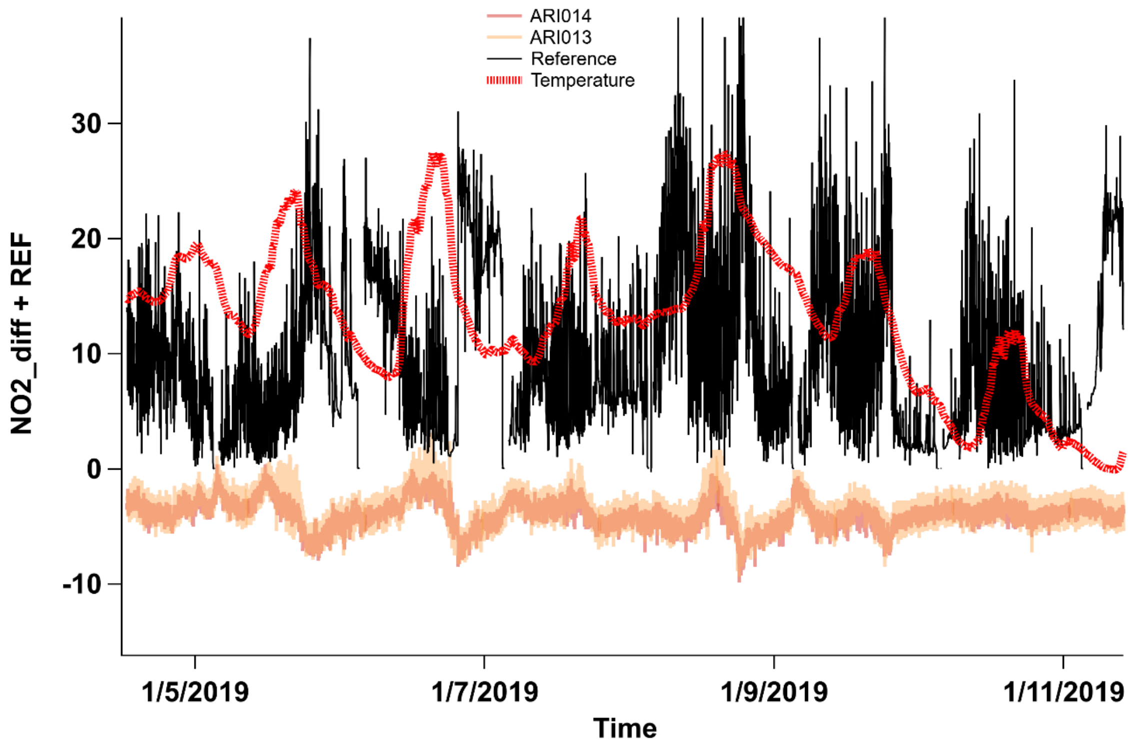

Figure S31: Time series of raw NO_2 differential voltage data from ARI013 and ARI014, NO_2 reference data (black), and temperature (red) during post-deployment collocation in North Carolina.

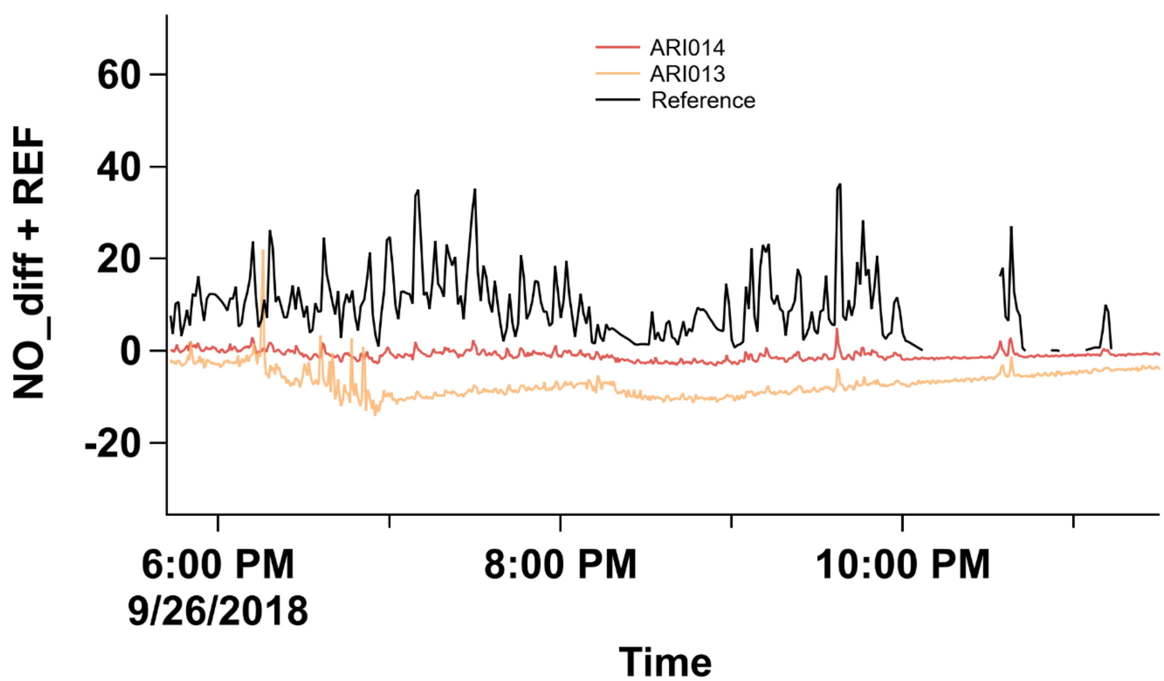

Figure S32: Time series of raw NO differential voltage data from ARI013 and ARI014 and NO reference data (black) during post-deployment collocation in North Carolina.

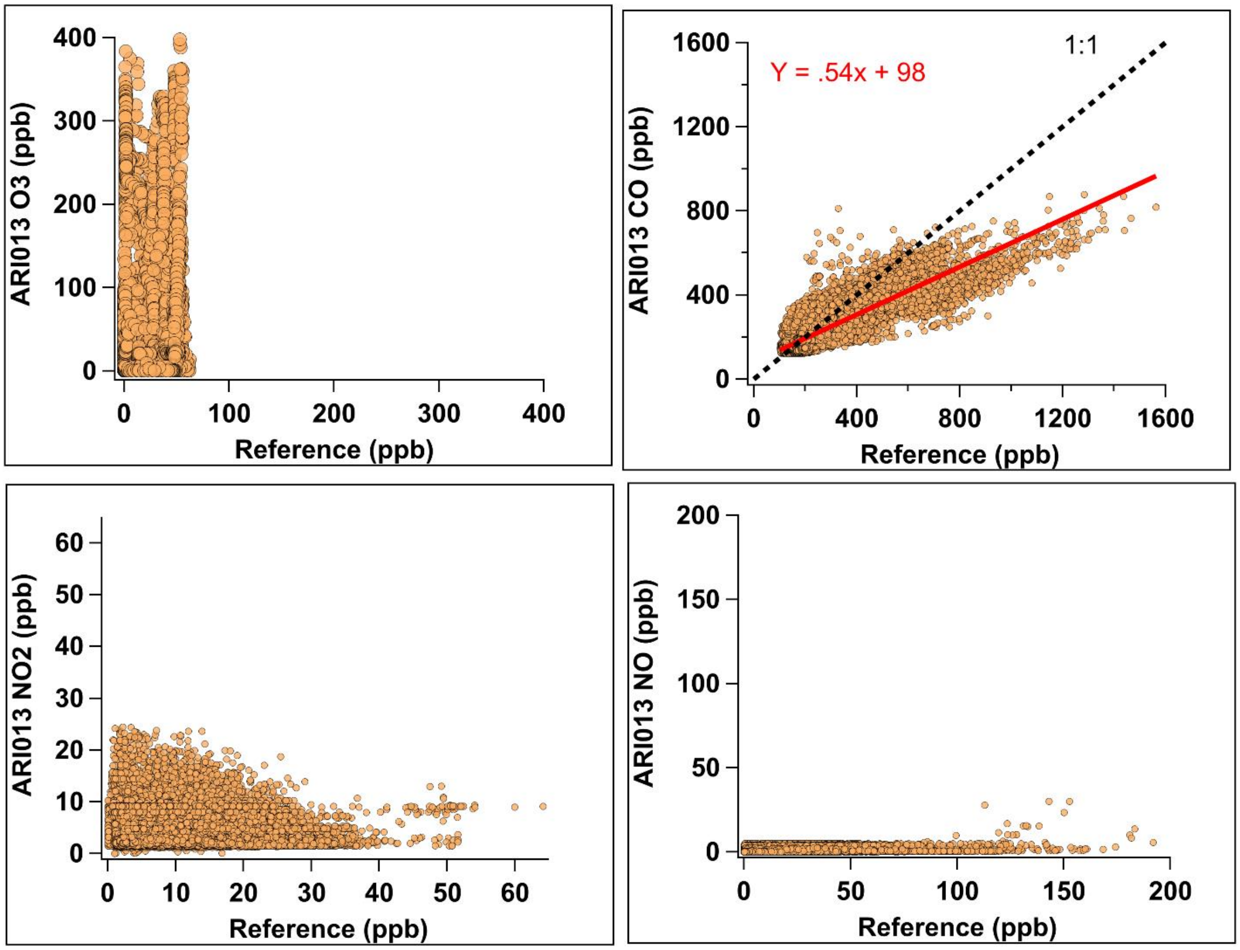

Figure S33: Scatter plots of kNN-calibrated data from each gas sensor in ARI013 (y-axis) compared to reference data (x-axis) during post-deployment collocation in North Carolina. Linear regression coefficients (y = mx + b), fit line (red line), the Coefficient of Determination (R^2) are shown for each paired comparison; A one to one comparison line is shown as the dotted black line.

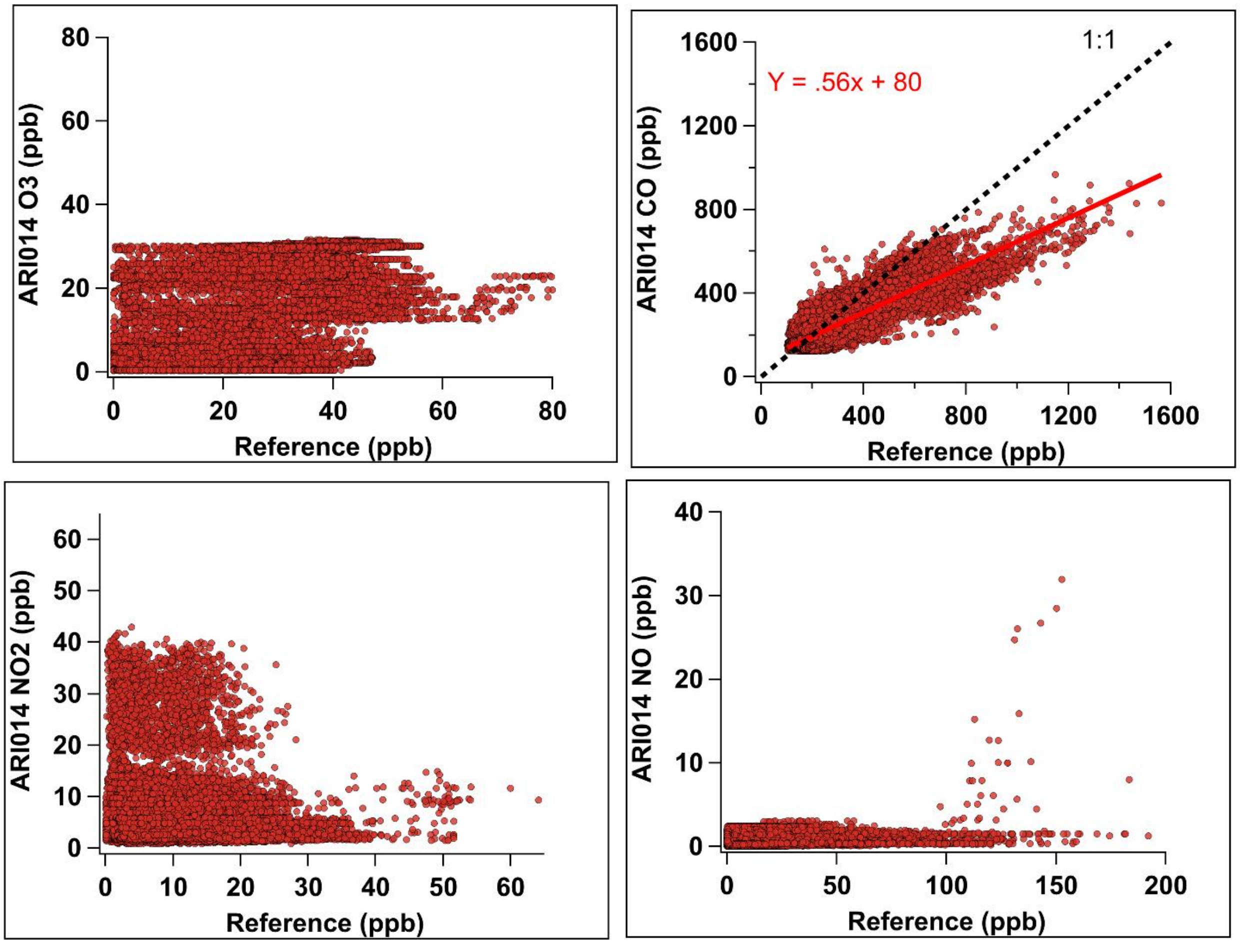

Figure S34: Scatter plots of kNN-calibrated data from each gas sensor in ARI014 (y-axis) compared to reference data (x-axis) during post-deployment collocation in North Carolina. Linear regression coefficients (y = mx + b), fit line (red line), the Coefficient of Determination (R^2) are shown for each paired comparison; A one to one comparison line is shown as the dotted black line.

References

Badura, M., Batog, P., Drzeniecka-Osiadacz, A., and Modzel, P.: Evaluation of Low-Cost Sensors for Ambient PM2.5 Monitoring, J. Sensors, vol. 2018, Article ID 5096540, 16 pages, https://doi.org/10.1155/2018/5096540, 2018.

Bean, J. K.: Evaluation methods for low-cost particulate matter sensors, 14, 7369–7379, https://doi.org/10.5194/amt-14-7369-2021, 2021.

Box, G. E. P. and Cox, D. R.: An Analysis of Transformations, J. Roy. Stat. Soc. B Met., 26, 211–252, 1964.

Bulot, F. M. J., Johnston, S. J., Basford, P. J., Easton, N. H. C., Apetroaie-Cristea, M., Foster, G. L., Morris, A. K. R., Cox, S. J., and Loxham, M.: Long-term field comparison of multiple low-cost particulate matter sensors in an outdoor urban environment, Sci. Rep-UK, 9, 7497, https://doi.org/10.1038/s41598-019-43716-3, 2019.

Champion, W. M. and Grieshop, A. P.: Pellet-fed gasifier stoves approach gas-stove like performance during in-home use in Rwanda, Environ. Sci. Technol., in press, acs.est.9b00009, https://doi.org/10.1021/acs.est.9b00009, 2019.

Crilley, L. R., Shaw, M., Pound, R., Kramer, L. J., Price, R., Young, S., Lewis, A. C., and Pope, F. D.: Evaluation of a low-cost optical particle counter (Alphasense OPC-N2) for ambient air monitoring, Atmos. Meas, Tech., 11, 709–720, https://doi.org/10.5194/amt-11-709-2018, 2018.

Duvall, R., Clements, A., Hagler, G., Kamal, A., Vasu Kilar, Goodman, L., Frederick, S., Johnson Barkjohn K., VonWald, I., Greene, D., and Dye, T.: Performance Testing Protocols, Metrics, and Target Values for Fine Particulate Matter Air Sensors: Use in Ambient, Outdoor, Fixed Site, Non-Regulatory Supplemental and Informational Monitoring Applications, U.S. EPA Office of Research and Development, Washington, DC, 2021a.

Duvall, R., Clements, A., Hagler, G., Kamal, A., Vasu Kilar, Goodman, L., Frederick, S., Johnson Barkjohn K., VonWald, I., Greene, D., and Dye, T.: Performance Testing Protocols, Metrics, and Target Values for Ozone Air Sensors: Use in Ambient, Outdoor, Fixed Site, Non-Regulatory and Informational Monitoring Applications, U.S. EPA Office of Research and Development, Washington, DC, 2021b.

Rai, A. C., Kumar, P., Pilla, F., Skouloudis, A. N., Di Sabatino, S., Ratti, C., Yasar, A., and Rickerby, D.: End-user perspective of low-cost sensors for outdoor air pollution monitoring, Sci. Total Environ., 607–608, 691–705, https://doi.org/10.1016/j.scitotenv.2017.06.266, 2017.